Ⓔ

WHITE DWARF SEQUENCES IN DENSE STAR CLUSTERS

Jarrod R. Hurley[1] and Michael M. Shara
Department of Astrophysics, American Museum of Natural History, Central Park West at 79th Street, New York, NY 10024;
jhurley@amnh.org, mshara@amnh.org

ABSTRACT

We use the results of realistic *N*-body simulations to investigate the appearance of the white dwarf population in dense star clusters. We show that the presence of a substantial binary population in a star cluster, and the interaction of this population with the cluster environment, has serious consequences for the morphology of the observed white dwarf sequence and the derived white dwarf cooling age of the cluster. We find that over time the dynamical evolution of the cluster—mass segregation, stellar interactions, and tidal stripping—hampers the use of white dwarfs as tracers of the initial mass function and also leads to a significant enhancement of the white dwarf mass fraction. Future observations of star clusters should be conducted slightly interior to the half-mass radius of the cluster in order to best obtain information about the cluster age and initial mass function from the white dwarf luminosity function. The evolution of binary stars and the cluster environment must necessarily be accounted for when the white dwarf populations of dynamically evolved star clusters are studied.

Subject headings: Galaxy: formation — globular clusters: general — methods: *n*-body simulations — open clusters and associations: general — stellar dynamics — white dwarfs

On-line material: color figures

1. INTRODUCTION

The technique of using the white dwarf (WD) sequence in the color-magnitude diagram (CMD) of a star cluster to derive a "cooling age" for the cluster is finally being exploited with ever increasing success (Richer et al. 1998; von Hippel & Gilmore 2000; Kalirai et al. 2001b; Andreuzzi et al. 2002; Hansen et al. 2002). This is largely due to the observational power of the *Hubble Space Telescope* (*HST*) and its ability to detect faint WDs. Credit must also go to the development of more sophisticated cooling models for WDs (e.g., Hansen 1999). Strong constraints, independent of cosmological models and parameters, are being placed, with this technique, on the age of the universe.

The determination of a *cooling age* for a star cluster is, as the term suggests, based on the fact that WDs cool systematically as they age, having only their residual ion thermal energy as a significant energy source. As a star cluster ages, its massive WDs form first from the most massive progenitors, and as time proceeds, progressively less massive WDs are introduced at the top of the WD cooling track. The more massive a WD is, the smaller it is (a consequence of being supported by electron degeneracy pressure) and the slower it cools. The net result is that as a star cluster evolves the WD cooling track moves redward in the CMD and that a blue *hook* develops as the older WDs are caught, in terms of decreasing luminosity, by younger (less massive) WDs. Furthermore, for any particular WD, its cooling rate initially decreases with time, and this causes the WDs to *pile up* at what is often referred to as the *bottom* of the cooling track. For older populations, such as globular clusters, the oldest WDs will actually lie below this point on the CMD because the cooling rate of a WD increases sharply in the later stages of its lifetime (after $\sim 9 \times 10^9$ Gyr depending on mass).

Regardless, we shall continue to refer to this point in the CMD as the *bottom* of the sequence, which is true at least for open clusters.[2] It is only with *HST*, and even then with extremely deep exposures, that the bottom of the WD cooling sequence in a globular cluster can be observed (Richer et al. 2002; Hansen et al. 2002). For nearby open clusters it is also possible to discover cool WDs by conducting deep photometric surveys using ground-based telescopes (Richer et al. 1998; Kalirai et al. 2001b). We note that the *blue hook* mentioned above is a mass effect and is not that described by Hansen (1998) in which an individual WD with a hydrogen-rich atmosphere evolves blueward in the CMD as it cools below 4000 K.

When the age of a cluster is calculated using observations of the WD sequence, the luminosity function (LF) can be utilized to varying degrees. The *clump-up* of WDs at the bottom of the cooling track corresponds to a maximum, or peak, in the WD LF. The presence of this feature in an observed LF for an open cluster is evidence that the oldest WDs have been uncovered (von Hippel, Gilmore, & Jones 1995). Then, by making assumptions about the mass and composition of these WDs, one can derive an age by using cooling models to find the time taken to cool to the absolute magnitude corresponding to the maximum in the LF (Richer et al. 1998; von Hippel & Gilmore 2000; Kalirai et al. 2001a). In fact, Brocato, Castellani, & Romaniello (1999) have shown theoretically that a unique relation exists between the faintest luminosity of a WD on the cooling sequence of an open cluster and the cluster age, as was first suggested by Schmidt (1959). For this age to be useful one must be sure that the true maximum in the LF has been

---

[2] The description of WD cooling presented here is necessarily simplistic. We suggest that the interested reader visit http://astro.ucla.edu/~hansen/m4.html, which includes a clickable WD sequence with explanations of the various features.

[1] Hubble Fellow.

observed, i.e., that the maximum is not produced by incompleteness. In the case of a globular cluster, or an open cluster if a large enough population of WDs is observed, the more sophisticated method of directly fitting the resulting LF can be applied (Andreuzzi et al. 2002). As an excellent example of the potential of this technique, Hansen et al. (2002) have used the WD sequence of the globular cluster M4 to demonstrate a clear age difference between this halo object and the Galactic disk. A robust lower limit to the age of M4 (and hence the universe) is found to be 12.7 ± 0.7 Gyr.

An indirect method for using cluster WDs to age the cluster comes from matching the WD sequence to the fiducial sequence obtained from local WDs with known trigonometric parallax and measuring the distance to the star cluster (Renzini et al. 1996; Zoccali et al. 2001). The distance can then be used to obtain the luminosity of the main-sequence (MS) turnoff in the CMD, and then an age can be calculated by comparison with stellar models. The determination of the WD mass fraction in a cluster is also of importance since it relates to the nature of the initial mass function (IMF) and the WD population of the Galactic halo (von Hippel 1998).

In light of the strong current interest being shown toward WDs in star clusters, we believe it is pertinent to discuss the theoretically expected behavior of these stars, in particular the morphology of the cluster WD sequence, from the point of view of realistic dynamical simulations. These same simulations have already been used to demonstrate that significant feedback exists between the dense stellar environment of a star cluster and the nature of its stellar populations (Hurley et al. 2001; Hurley & Shara 2002b; Shara & Hurley 2002). In this paper we show that the same is true for the cluster WD population but that this does not necessarily affect the derived cooling age of a cluster. However, we find

that extreme care must be taken when using cluster WDs to make inferences about the IMF, when using either the WD luminosity function or the WD mass fraction.

In § 2 we describe the realistic N-body models, including stellar evolution, used to simulate WD cooling sequences of star clusters. We discuss the appearance of these sequences in § 3 and investigate the role of mass segregation in § 4. We then establish to what extent the LF and the mass fraction of the WD population is affected by the cluster evolution, in §§ 5 and 6, respectively, before providing a discussion and summary of our findings.

2. THE N-BODY SIMULATIONS

We present results from N-body simulations performed with the Aarseth NBODY4 code (Aarseth 1999) on the GRAPE-6 special-purpose computers (Makino & Taiji 1998) housed at the American Museum of Natural History. The NBODY4 code accounts for the evolution of single stars and binaries (mass loss, mass transfer, mergers, etc.) while modeling all aspects of the dynamical evolution of the cluster (see Hurley et al. 2001 and references therein for full details). In particular, the single-star evolution algorithm adopted by NBODY4 is that of Hurley, Pols, & Tout (2000). This algorithm models the luminosity evolution of WDs using standard cooling theory (Mestel 1952), and the radius of a WD is calculated from equation (17) of Tout et al. (1997). The stellar evolution algorithm distinguishes three types of WD based on the core composition of the giant precursor: helium, carbon-oxygen (CO), or oxygen-neon (ONe). The CO WDs are 20% carbon and 80% oxygen, while the ONe WDs are 80% oxygen and 20% neon (note that neon is representative of all carbon-burning products heavier than oxygen). Figure 1 compares the cooling
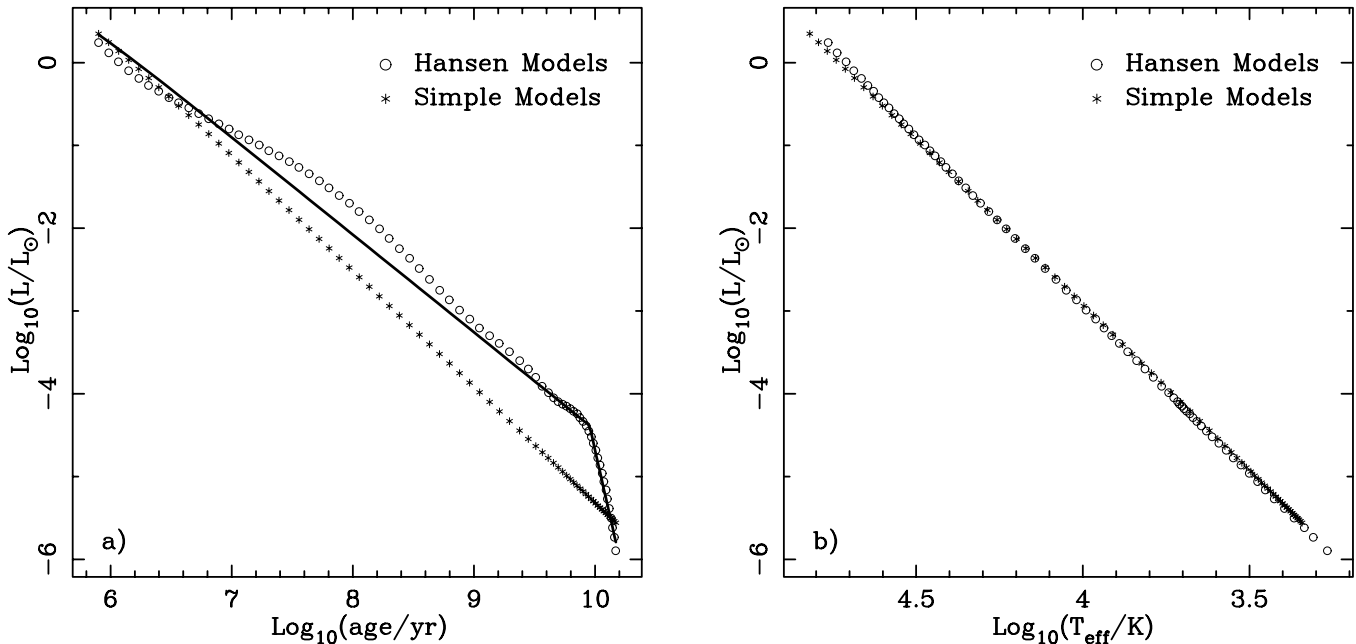

FIG. 1.—Comparison of the Hansen (1999) detailed cooling models with the simple cooling track adopted by Hurley et al. (2000), using a 0.7 $M_\odot$ WD as an example. *Left:* Evolution of luminosity with time. *Right:* Hertzsprung-Russell diagram. The radius of the Hansen (1999) WD decreases from $\log(R/R_\odot) = -1.88$ to -1.96 in the first 500 Myr of cooling and remains approximately constant from that point onward. The radius of the Hurley et al. (2000) model is held constant at $\log(R/R_\odot) = -1.94$ throughout. Also shown in the left panel (*solid line*) is the evolution of the luminosity with time for the modified Mestel law used in this paper (see text for details). Note that at late times the solid line is hidden by the Hansen (1999) model points.

track of a 0.7 $M_\odot$ CO WD evolved with the Hansen (1999) models with the rather simplified model of Hurley, Pols, & Tout (2000). As noted by Iben & Tutukov (1984), the Mestel theory assumes that a WD is basically an isothermal core composed of an ideal ionic gas embedded in an electron-degenerate gas and that this is surrounded by a thin envelope through which photons diffuse at a rate governed by Kramers opacity. In Figure 1 the decreased cooling rate shown by the Hansen (1999) WD at early times is explained by the inclusion of neutrino cooling and true atmospheric opacities in the detailed models. As the WD cools a number of processes neglected by the simple model become important: crystallization of ions in the core, the release of latent heat, and the rise of convection as a transport mechanism. At late times the crystalline core enters the Debye regime and there is a sharp increase in the cooling rate (B. Hansen 2002, private communication). To address the differences between the WD cooling rate of the Mestel theory and of the Hansen (1999) detailed models we have constructed a *modified* Mestel cooling law. The original Mestel cooling law can be expressed as

$$L = \frac{bM_{\mathrm{WD}}Z^{0.4}}{[A(t+0.1)]^x} \, , \tag{1}$$

where the factor $b = 635$, the exponent $x = 1.4$, M_{WD} is the mass of the WD in solar units, Z is the metallicity, A is the baryon number for the WD material, and t is the age of the WD in Myr. For our modified Mestel law we split this relation into two parts: we use $b = 300$ and $x = 1.18$ for $t < 9000$ Myr and $b = 300(9000A)^{5.3}$ and $x = 6.48$ for $t \geq 9000$ Myr. As can be seen from Figure 1 this rather ad hoc relation provides a much better fit to the detailed models, especially after noting that the accuracy of the Hansen (1999) models increases for $t > 10^8$ yr (B. Hansen 2002, private communication). The modified Mestel cooling law has been inserted into NBODY4 and is used throughout this work. This provides an initial *qualitative* assessment of the theoretically expected character of cluster WD cooling sequences. However, in the near future we will want to directly compare the WD sequences and LFs emerging from the *N*-body data with observations, and for this it will be important to obtain a more sophisticated fit to the behavior of the realistic WD models (as soon as a full database of such models becomes available). Metallicity variations are generally neglected in the construction of detailed WD cooling models because the strong surface gravity of a WD will cause all elements heavier than helium to sink below the atmosphere (Hansen et al. 2002). We note that the Mestel cooling law does contain a weak dependence on Z through the assumption of electron scattering for the atmospheric opacity.

We focus on the results of three simulations that each started with 28,000 stars and a primordial binary frequency, f_b, of 40%, i.e., 12,000 single stars and 8000 binaries. The IMF of Kroupa, Tout, & Gilmore (1993) was used to assign the masses of single stars, and a metallicity of $Z = 0.02$ was assumed. For primordial binaries the total mass of the binary was chosen from the IMF of Kroupa, Tout, & Gilmore (1991), since this was not corrected for the effect of binaries, and the component masses were then assigned according to a uniform mass ratio, q, distribution. Individual stellar masses were restricted to lie within the limits of 0.1–50 $M_\odot$. The orbital separation of each primordial

binary was taken from the lognormal distribution given by Eggleton, Fitchett, & Tout (1989), within the limits of 6 $R_\odot$ to 200 AU,[3] and the orbital eccentricity was taken from a thermal distribution (Heggie 1975). We used a Plummer model (Aarseth, Hénon, & Wielen 1974) in virial equilibrium to set the initial positions and velocities of the stars but note that the density profile quickly evolved to resemble a King model (King 1966). The simulated clusters were assumed to be on a circular orbit within a Keplerian potential with a speed of 220 km s^{-1} at a distance of 8.5 kpc from the Galactic center. Stars were removed from the simulation when their distance from the cluster center exceeded twice the tidal radius defined by this tidal field. All stars were on the zero-age main sequence (ZAMS) when the simulation began, and any residual gas from the star formation process is assumed to have already left the cluster. Mass lost from stars during the simulation is simply removed from the cluster, with the cluster potential adjusted accordingly.

Each cluster started with a total mass of $\sim$14,300 $M_\odot$ and was evolved to an age of 6 Gyr, at which point $\sim$1000 $M_\odot$ in stars remained. The initial velocity dispersion of the stars was $\sim$3.2 km s^{-1} (reduced to $\sim$1 km s^{-1} after 6 Gyr), and the core density was $\sim$500 stars pc^{-3}. The average number density of stars in the core throughout the simulations was 200 stars pc^{-3}. The density within the radius that contained the inner 10% of the cluster mass started at the same value, reached a minimum of 50 stars pc^{-3} after $\sim$4 Gyr, and rose to 100 stars pc^{-3} at 6 Gyr. Each simulated cluster showed a modest core collapse at $\sim$1 Gyr, identified by a significant increase in core density, but we note that for models with such a large proportion of primordial binaries the exact point of core collapse is difficult to judge, if it occurs at all.

For reference purposes we have performed two additional simulations that each started with 28,000 stars but no primordial binaries. We also draw upon the simulations with 20,000 stars and $f_b = 10\%$ described by Shara & Hurley (2002) in their work on double-WD binaries in star clusters. As a result, our findings are directly applicable to intermediate-mass and massive open clusters. By making the appropriate scalings we can (cautiously) make inferences relating to WDs in globular clusters as well. More realistic, $N \geq 10^5$, simulations will be needed to make definite predictions about globular clusters.

3. THE WHITE DWARF SEQUENCE

We have chosen to concentrate on the simulated cluster data at 4 Gyr for the purpose of illustrating the nature and appearance of the cluster WD population. There are a number of reasons for this choice. First, this is late enough in the simulation (approximately 12 half-mass relaxation times have elapsed) that the cluster is dynamically evolved. On the other hand, it is not so late that the number counts of the stellar populations have become statistically insignificant. Furthermore, if time is scaled by the half-mass relaxation timescale, t_{rh}, then an age of 4 Gyr for a cluster of $\sim$30,000 stars is representative of a 100,000 star cluster at 12 Gyr

---

[3] The third simulation had an upper limit of 50 AU, but this still exceeds the hard/soft binary limit for simulations of this size. According to Heggie (1975), it is only initially hard binaries that will contribute to the long-term evolution of the cluster. We note that in this case the primordial binary population is effectively representative of a larger population drawn from a full range of separations.
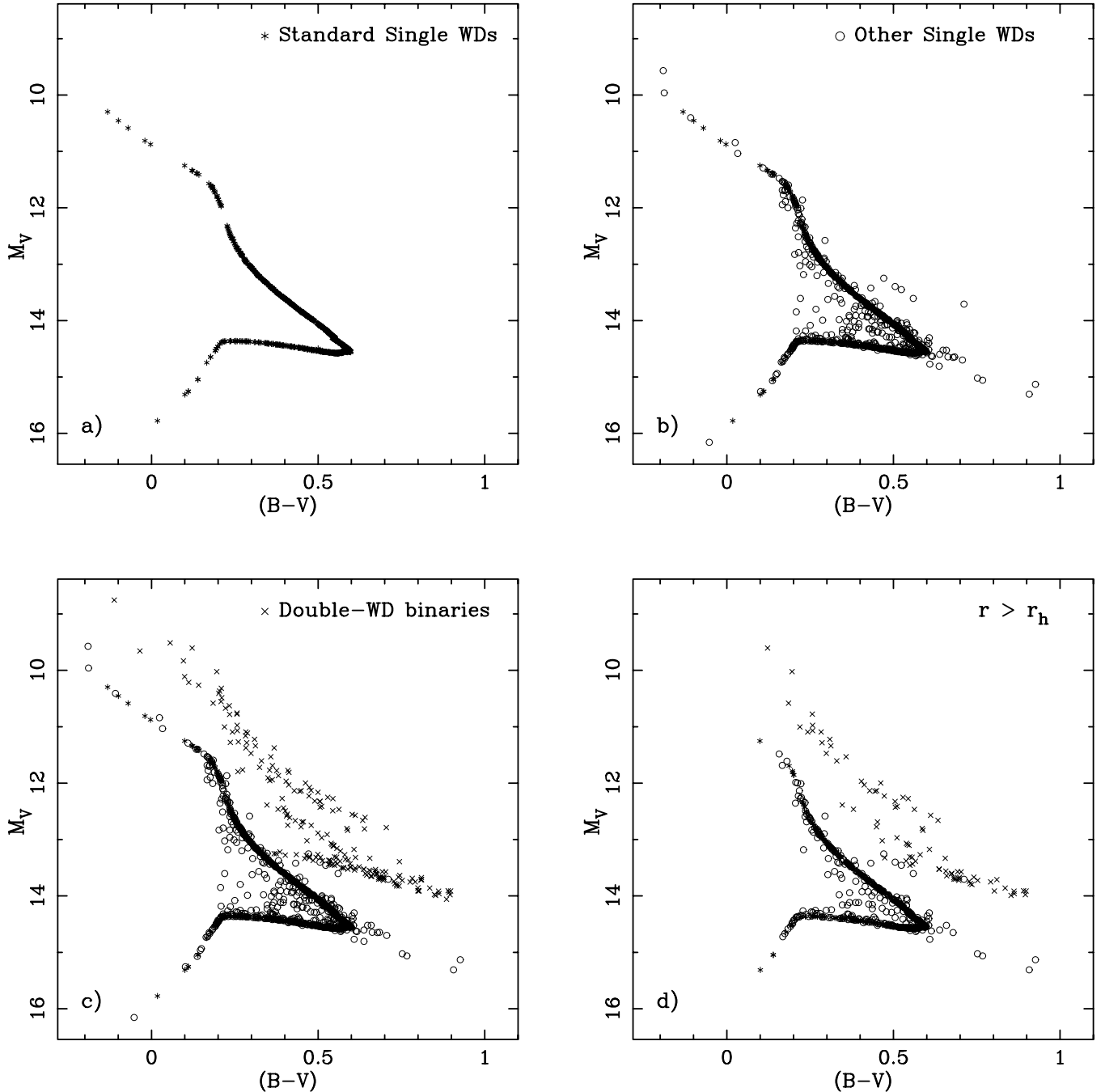
Fig. 2.—Cluster CMD for WDs at 4 Gyr. Stars from three *N*-body simulations, each with $N_0 \simeq 28,000$ and $f_b \sim 40\%$, are shown. All WDs are assumed to be of DA type, and bolometric corrections are taken from Bergeron, Wesemael, & Beauchamp (1995). We have distinguished three different types of WDs depending on their binarity and formation path: single WDs that evolved from single stars (standard), single WDs for which the progenitor star (or stars) was previously the member of a binary, and double-WD binaries. Note that all binaries are assumed to be unresolved. Panel (*a*) shows only the standard WDs, (*b*) adds in the remaining single WDs, and (*c*) shows all three types. (*d*) Same as (*c*) but showing only WDs that lie outside the cluster half-mass radius (typically 4.5 pc). There are a total of 863 standard WDs, 598 single WDs that evolved via a binary phase, and 198 double-WD binaries (25% of these formed via an exchange interaction).

(Meylan & Heggie 1997); *i.e., the results of our massive open cluster simulations at* 4 Gyr *can be related to a moderate-size globular cluster*. We regard this final point with some caution because a number of timescales are at work in a star cluster and these scale differently with *N* (Aarseth & Heggie 1998). It has also been shown that many of the structural properties of a star cluster are *N*-dependent (Goodman 1987).

Figure 2 shows the CMD at 4 Gyr for all WDs in the three $N = 28,000$ simulations with primordial binaries. To convert the theoretically derived quantities of luminosity and effective temperature to magnitudes and colors we have used the bolometric corrections provided by the WD models of Bergeron, Wesemael, & Beauchamp (1995). We start in Figure 2*a* by plotting only what we call standard single WDs. By this we mean that each of the WDs, and their

progenitor stars, were never part of a binary or involved in a collision and have evolved according to the standard picture of single-star evolution. This produces the smooth cooling track seen in Figure 2a. For these WDs it is true that the more advanced along the track that a particular WD is, the more massive and older it is. We highlight the standard single WDs because these are the objects that the cooling models used to age the WD sequence directly relate to.

Next we add in all the remaining WDs that are single at 4 Gyr but whose progenitor was originally a member of a binary (Fig. 2b). Even though a substantial fraction of these WDs overlie the standard cooling track, it is evident that the remainder contribute a great deal of scatter to the CMD. As an example, some of these WDs have evolved from blue stragglers, or more generally any MS star rejuvenated by mass transfer. These progenitors' journeys to the asymptotic giant branch have been delayed; hence, when the WD was born it was more massive than WDs born from standard single stars at that time. This yields WDs lying below the standard WD sequence. Conversely, WDs less massive than expected at birth are produced from giants initially in binaries that overfilled their Roche lobe and lost their envelopes prematurely and then lost their partners in exchange interactions.

In Figure 2c we complete the full WD CMD by including all the double-WD binaries present at 4 Gyr. The first thing to notice is that for the most part the double-WD sequence is well separated from the standard cooling track. This is because the computed double-WD binaries are mainly high mass ratio systems (see Fig. 3), in agreement with the measured mass ratios of local double WDs (Maxted, Marsh, & Moran 2002). Provided that photometric errors are modest (say, ≤ 0.5 mag), it is possible to minimize contamination of the WD sequence by double WDs in at least the upper half of the WD CMD. Farther down the sequence we notice that
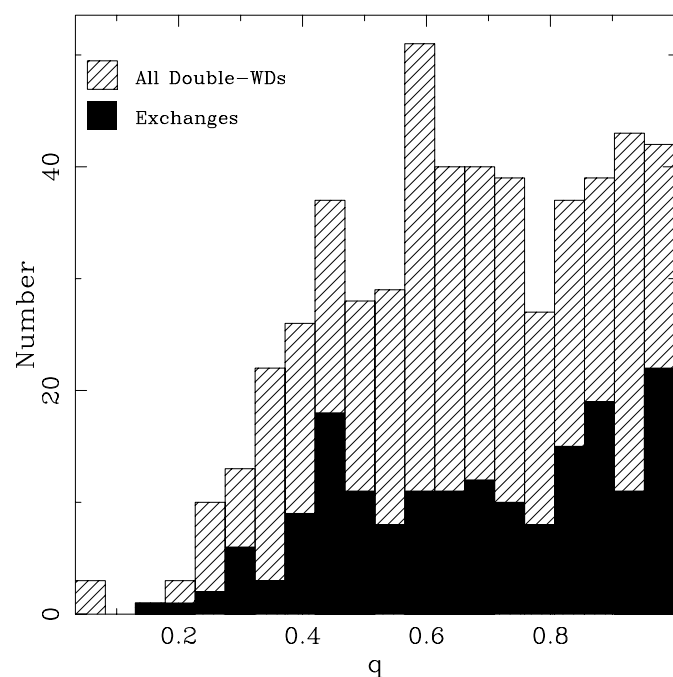
double WDs clump up at brighter magnitudes than do the single WDs and start to approach the WD sequence. This, combined with the scatter produced by the nonstandard single WDs, leads to our first note of caution regarding observations of cluster WD sequences. *Estimating the position of the bottom of the cooling track by the detection of WDs blueward of the track, or by a buildup of WDs at a certain magnitude, can be seriously misleading.* It is possible to just be seeing the scatter in the WD sequence produced by nonstandard WD evolution, or by a population of old double WDs, and one may need to go deeper to find the true extent of the track. If the termination of the double-WD sequence were to be mistakenly used as the bottom luminosity of the WD sequence, then, using the relation given by Brocato et al. (1999), this would translate to underestimating the cluster age by 1.6 Gyr for a cluster with an actual age of 4 Gyr.

In producing the WD CMD we have assumed that all the WDs are hydrogen-line (DA) type, whereas a small, but significant, fraction will actually have strong helium (DB), or other anomalous, features. At least 75% of spectroscopically identified WDs are classified as DA in the catalog of McCook & Sion (1999), but we note that for cool WDs the DA : DB ratio is more likely 1 : 1 (Bergeron, Ruiz, & Leggett 1997; Hansen 1999). Modeling of WDs that do not have pure hydrogen atmospheres will produce additional scatter in the WD CMD, as will other factors that affect the cooling times and temperatures of WDs: the relative fractions of carbon and oxygen in the interiors of CO WDs (Koester 2002) and the mass of the hydrogen (or helium) envelope (Hansen 1999), for example. Importantly, our simulations have been performed with moderate stellar density—at least an order of magnitude less than conditions within the core of an actual globular cluster—and at higher density the incidence of stellar interaction is expected to be higher, and hence a greater number of nonstandard single WDs will be produced.[4] Counteracting this, globular clusters are observed to have smaller binary fractions than used in our simulations: M4 has a binary frequency that could be as high as 15% (Côté & Fischer 1996) or as low as 4% (Richer et al. 1996). It is also possible that a higher stellar density may hinder the production of certain populations, such as double WDs, and lead to less contamination of the WD sequence.

Outside the half-mass radius, r_h, of a star cluster the number density of stars is less than in the core and the incidence of stellar interactions is also less. The binary fraction is also smaller in this region because mass segregation is effective in causing binaries to sink toward the cluster center (see § 4). These considerations lead to a much cleaner WD sequence, as shown in Figure 2d, and it is here that observations of WD sequences (for the purposes of age dating) in globular clusters can most cleanly be conducted, if enough WDs are present.

Shara & Hurley (2002) found that open star clusters produce supra–Chandrasekhar mass double-WD binaries with merger timescales less than a Hubble time at a greatly enhanced rate relative to the field. Of the 198 double WDs shown in Figure 2, 35 have a combined mass in excess of the

Fig. 3.—Mass ratio, q, distribution of double white dwarfs present in an N-body simulation at 4.0 Gyr. Note that we define q so that it is always less than unity.

---

[4] For example, the high-density globular cluster M80 is observed to have a large number of blue stragglers in its core (305; Ferraro et al. 1999) and therefore would be expected to also contain a large number of nonstandard WDs.
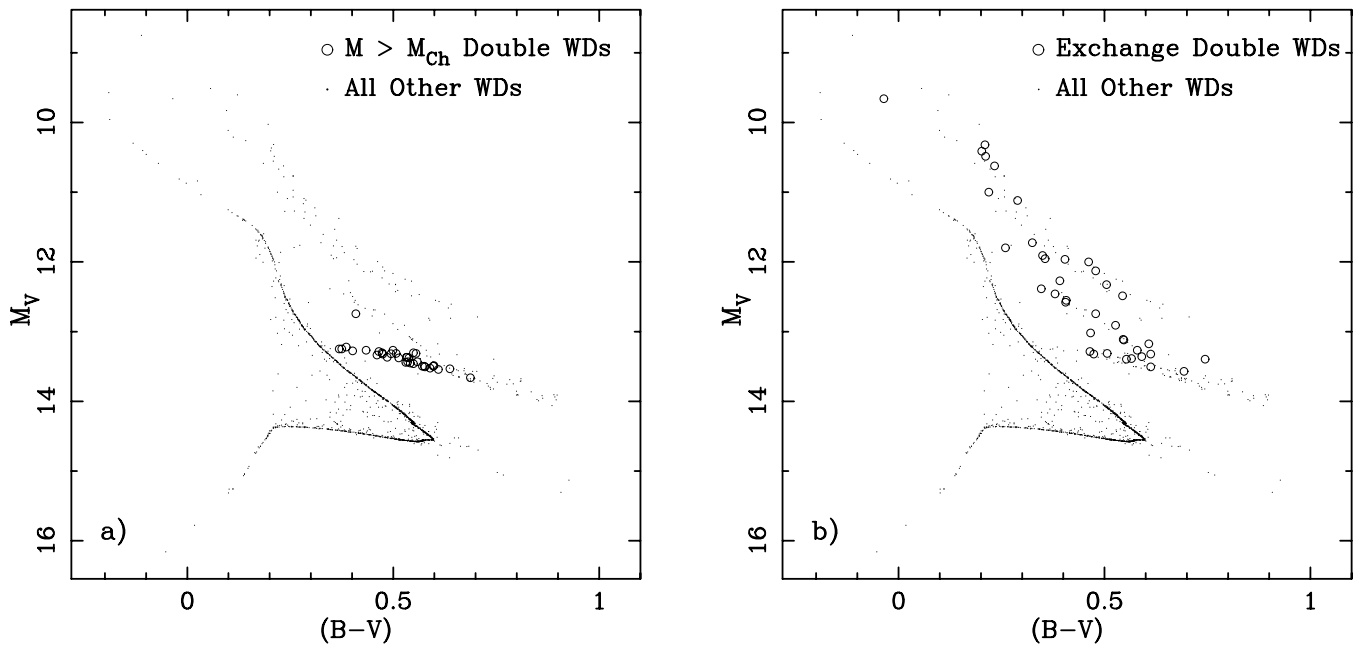
Fɪɢ. 4.—Same as Fig. 2c but distinguishing double-WD binaries that have a combined mass in excess of the Chandrasekhar limit for a single WD (*left*) and double-WD binaries that formed via an exchange interaction (*right*).

Chandrasekhar mass, and these are highlighted in Figure 4 (*left panel*). All but two of the supra–Chandrasekhar mass double WDs lie in a clump just to the right of the standard single-WD sequence. The area defined by this clump also contains 12 other stars (nonstandard single WDs and sub–Chandrasekhar mass double WDs), which means that 73% of the stars in this subarea of the CMD are supra–Chandrasekhar mass double WDs. Provided that observations can be performed with suitably high signal-to-noise ratio, this method is a possible way to isolate these potentially interesting binaries. More sophisticated follow-up methods, such as the use of a gravitational wave detector (Benacquista 1999), would be required to learn about the merger timescales of these binaries. Figure 4 (*right panel*) also highlights the double-WD binaries produced by exchange interactions during the simulations: 25% of the double-WD binaries at 4 Gyr are nonprimordial. It can easily be seen that these binaries do not preferentially form in any particular subarea of the general double-WD sequence (see also Fig. 3), and hence they cannot be isolated by photometric methods.

4. MASS SEGREGATION

A number of N-body studies (Giersz & Heggie 1997; Portegies Zwart et al. 2001; Hurley et al. 2001; Hurley & Shara 2002a) have previously verified the Fokker-Planck results of Chernoff & Weinberg (1990): mass segregation occurs in star clusters, and this causes stars less massive than the average stellar mass to migrate outward on a timescale governed by two-body relaxation. Conversely, stars more massive than average sink toward the center of the cluster. Low-mass stars are thus preferentially stripped from the cluster by the external potential of the Galaxy. To reinforce these findings we show in Figures 5a and 5b population gradients for single stars, WDs, and double WDs at 1 and 4 Gyr, respectively. Clearly, the WDs are more centrally concentrated than the overall population of single stars, and there-

fore it is less likely that WDs will be lost from the cluster by tidal stripping. In fact, for our $N = 28,000$, $f_b = 40$% simulations after 4 Gyr of evolution, 20% of the mass generated in WDs has escaped from the cluster, with the average mass of these WD escapers being $\sim 0.7 \ M_\odot$. By contrast, 91% of the mass in single MS stars with $M < 0.7 \ M_\odot$ has been lost from our models after the same period of time. After 1 Gyr only 4% of the WD mass has escaped from the cluster. The fraction of mass lost from the cluster in escaping WDs agrees favorably with Vesperini & Heggie (1997) in comparison with their model at 8 kpc from the Galactic center after a similar number of relaxation times have elapsed.

Some central concentration of the WD population is to be expected because their average mass is greater than that of all the cluster stars (for $t < 5$ Gyr; see Fig. 5c). However, the main reason for this concentration is that the progenitors of the WDs were originally more massive than the current MS turnoff mass and therefore the WDs are more likely to be born interior to r_h. This point was also discussed by Portegies Zwart et al. (2001) in relation to their $N = 3000$ models of young open clusters. Binaries are on average more massive than single stars and as such will segregate toward the center of the cluster. This is also true of double-WD binaries (see top panels of Fig. 5), which have an even higher average mass than standard binaries.

Figure 5c shows the average mass of the WDs as a function of time, and also the average mass of all the single stars in the cluster, excluding WDs and other degenerate objects. The single-star average mass initially decreases owing to mass loss from the most massive stars but then begins to increase as tidal stripping of low-mass stars slowly starts to dominate over mass loss from stellar evolution. If the cluster was instead evolved in isolation so that tidal stripping was not accounted for, then the single-star average mass at 4 Gyr would be 0.36 $M_\odot$ as opposed to 0.51 $M_\odot$. The reverse is true for the evolution of the WD average mass—stellar evolution and not tidal stripping is the dominant factor.
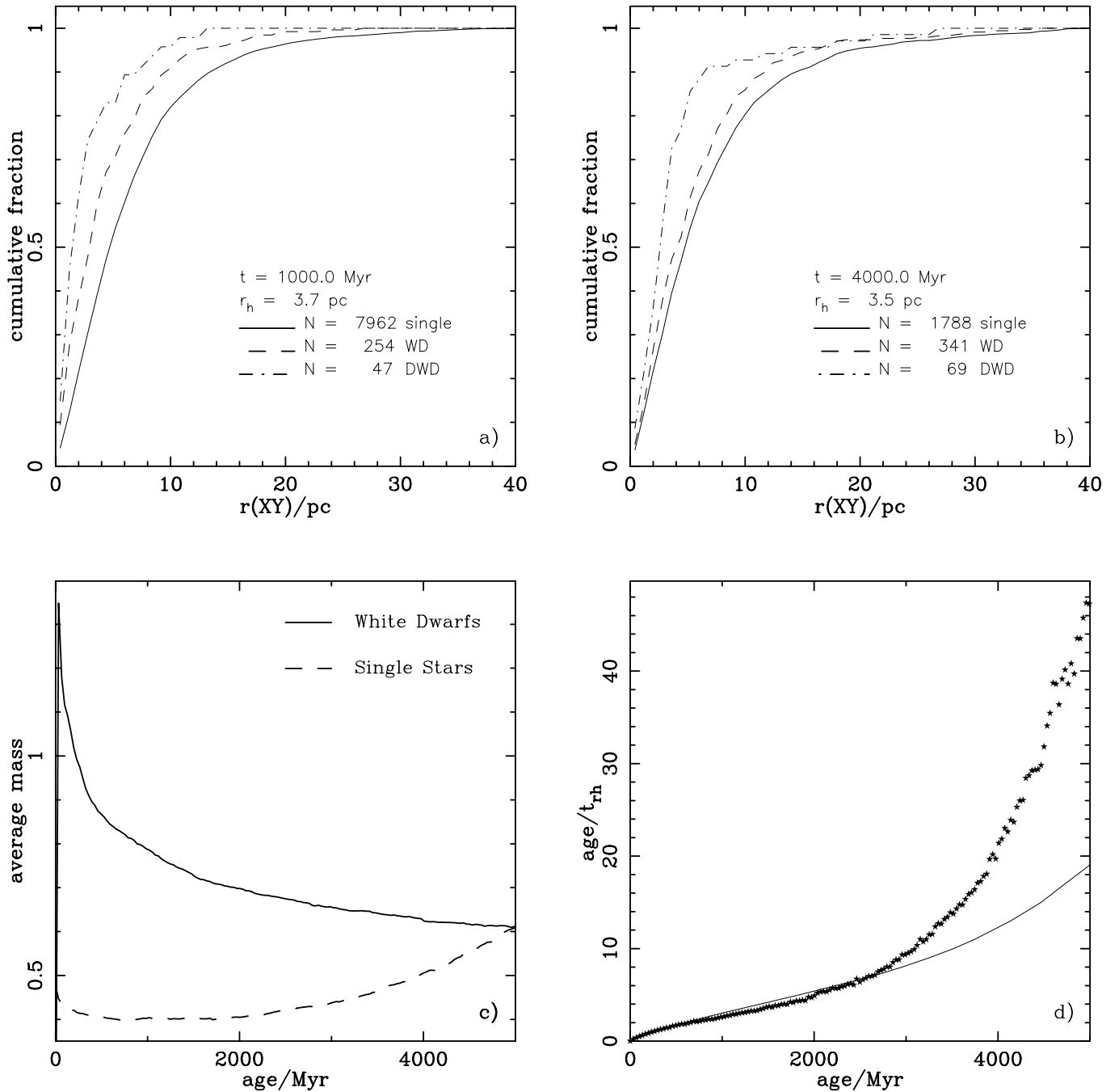
Fig. 5.—*Top:* Cumulative radial distributions of single stars, single WDs, and double-WD binaries at ages of 1 Gyr (*top left*) and 4 Gyr (*top right*). Also shown, as a function of time, is the evolution of the average stellar mass for WDs and non-WD single stars (*bottom left*) and the cluster age scaled by the half-mass relaxation timescale, t_{rh}, current at that time (*bottom right*; the solid line represents the number of actual half-mass relaxation times elapsed by using the integrated half-mass relaxation timescale). Data from the three simulations with $N \sim 28,000$ and $f_b \sim 40\%$ are included.

The first WD forms at ~ 40 Myr from a star with a ZAMS mass of 8 $M_\odot$ and is of oxygen-neon composition with a mass slightly below the Chandrasekhar mass (1.44 $M_\odot$). Then, as time proceeds, the zero-age WD mass progressively decreases (see Hurley, Pols, & Tout 2000 for a full description of the WD initial-final mass relation generated by the evolution algorithm), which eventually results in a buildup of CO WDs with masses in the range 0.6–0.7 $M_\odot$. Helium composition WDs are also produced but only after some form of binary interaction. These have an average mass of 0.34 $M_\odot$. The average WD mass at 4 Gyr is 0.62 $M_\odot$, practi-

cally the same as it would be if the population had been evolved in isolation. While the single-star average mass is sensitive to where in the cluster it is measured, decreasing from 0.82 $M_\odot$ in the core to 0.37 $M_\odot$ near the tidal boundary at 4 Gyr, the WD average mass is relatively uniform throughout the cluster. Thus, it would appear that overall the WD population has been little affected by the dynamical evolution of the cluster, in agreement with the conclusion of Portegies Zwart et al. (2001), although we show in the next section that this is not necessarily true when considering the WD LF.

The fact that over time the progenitor mass of the WDs is steadily decreasing and that the WD and single-star average masses are nearing equality explains why the WDs appear marginally less centrally concentrated at 4 Gyr than at 1 Gyr. Eventually, the average mass of the nondegenerate single stars will increase above that of the WDs and the population gradients of the two populations will converge, mainly as a result of the WDs drifting slowly outward. However, by the time this occurs the cluster is dynamically very old—in excess of 20 half-mass relaxation times will have elapsed—and near complete disruption.

In Figure 5d we show how the cluster age scales with the half-mass relaxation timescale because this can be a useful reference tool for interpreting the results of the simulations. We show the number of half-mass relaxation times elapsed both when simply dividing the cluster age by the current t_{rh} and when integrating t_{rh} over the lifetime of the cluster. The latter number is representative of the true dynamical age of the cluster, and the two methods give similar results until t_{rh} starts to decrease during the latter stages of evolution. The half-mass relaxation timescale for the simulations starts at $\sim$200 Myr, rises to $\sim$450 Myr at 2 Gyr, and has decreased back to $\sim$200 Myr after 4 Gyr of evolution. It basically follows the evolution of the cluster half-mass radius, which increases initially owing to mass loss from massive stars and then decreases as it starts to feel the effect of the shrinking tidal radius (Hurley et al. 2001). At 4 Gyr, $r_h = 4$ pc for these simulations.

5. THE LUMINOSITY FUNCTION

The WD luminosity function holds information about the age of a cluster and the IMF of its stars. In order to extract this information accurately, we must be sure that the observed WD LF is relevant for the intended purpose. For the age determination this really boils down to being certain that the true peak in the LF has been identified. In the case of open clusters this corresponds to being certain that the *bottom* of the WD sequence has been reached, i.e., that the coolest standard single WD has been observed. However, for the older populations of globular clusters it is not yet possible to observe the oldest WDs because these will be massive helium atmosphere WDs with luminosities below current detection limits (Hansen 1999). The attraction of this approach is that it provides an age that is relatively independent of stellar evolutionary models because the nuclear burning lifetime of the progenitor to the oldest WDs is short ($\sim$40 Myr) compared to the age of all globular clusters and most open clusters (von Hippel et al. 1995). For the case of inferring the IMF we must be sure that the observed WD LF is a true representation of the present-day mass function (PDMF) of the cluster, noting that for WDs the LF and MF are directly related via the cooling models.

In Figure 6 we show the WD LF from the *N*-body simulations at 4 Gyr for the entire WD sequence (as shown in Fig. 2c). We also show the LF for the standard single WDs. Performing a χ^2 test reveals a probability of 0.02 that the two LFs are drawn from the same distribution. The main points to notice are that contamination of the WD sequence by the presence of double WDs and nonstandard single WDs does not affect the location of the LF maximum but that the slope of the LF *is strongly* affected.
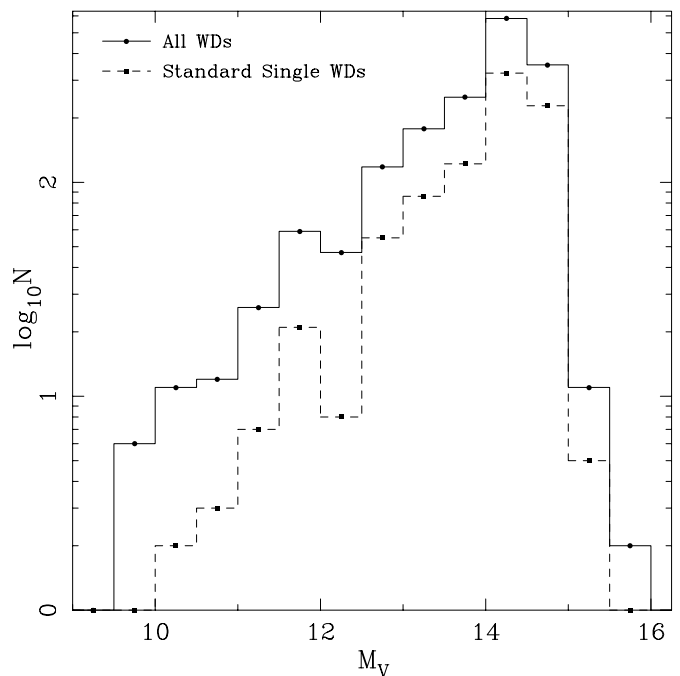

FIG. 6.—WD luminosity functions at 4 Gyr for all WDs (*solid line*) and for single WDs that evolved from single stars (*dashed line*). WDs from all three simulations with $N \sim 28,000$ and $f_b \sim 40\%$ are included. The LF for all WDs (which includes double-WD binaries) is best fitted across the range of masses that produce WDs for $t \leq 4$ Gyr (1.4–8.0 $M_\odot$ for $Z = 0.02$) by a Salpeter (1955) IMF with slope $\alpha = 3.75$. The LF for standard single WDs is best fitted by a Salpeter (1955) IMF with slope $\alpha = 3.15$.

5.1. *Inferred IMF Slopes*

For a population with $Z = 0.02$ at an age of 4 Gyr the range of ZAMS stellar masses that will have evolved to become WDs is 1.4–8.0 $M_\odot$. Assuming a power-law IMF of the Salpeter (1955) form (where $\alpha = 2.35$ is the corresponding slope of the function in our chosen notation), we can fit the IMF slope in this mass range to the cluster LF by constructing theoretical LFs for a range of α. In this case the LFs from the *N*-body simulations are the *observed* LFs. When constructing the theoretical LFs we evolve only single stars because we want to quantify how the inclusion of nonstandard WDs in the LF affects the inferred IMF. These single stars are evolved according to the same rapid-evolution algorithm used by NBODY4. This ensures that uncertainties in the accuracy of the WD cooling tracks and the MS lifetimes of the WD progenitors, for example, do not play a role in the fitting process. No dynamical effects are accounted for in the theoretical LFs. To determine the appropriate α for an observed LF we find the theoretical LF that gives the smallest value of the χ^2 statistic, where we have used $\Delta\alpha = 0.05$ in constructing the theoretical LFs. The two distributions are normalized so that the sums of all bins are equal, which means that the number of degrees of freedom in the fitting process is one less than the number of bins. We note that the probability returned by the χ^2 fit is not independent of the normalization—if the distributions are normalized to a greater total number of WDs, the probability that the fit is a good one decreases (for the same number of bins). In this work we are primarily concerned with using the value of χ^2 to determine which α gives the best fit. However, the probability returned by the fit may also be of

interest, so we have made sure to use the same normalization throughout this work; i.e., all distributions are normalized to have the same total number of WDs as that given by the solid line in Figure 6 before commencing the fitting process.

The result is $\alpha = 3.75$ (with a probability of 0.30 that this is a good fit) when we consider all the WDs and $\alpha = 3.15$ (0.65) for the standard single-WD LF. We note that the slope of the Kroupa et al. (1993) IMF used in these simulations is 2.7 for masses in excess of 1 $M_\odot$, and therefore, after 4 Gyr of evolution, the standard single WDs are no longer representative of the true PDMF for the initial population (evolved without dynamics). After 1 Gyr the LF for standard single WDs is best fitted by $\alpha = 2.70$ (0.87), and after 2 Gyr the fit reveals $\alpha = 2.80$ (0.76)—further evidence that over time the cluster environment is eroding the usefulness of the WDs as tracers of the IMF but also showing that it takes time for this erosion to become significant. The presence of double WDs in the LF increases the relative number counts in the intermediate-magnitude bins (located in the range of ~1–3 mag below the peak), effectively *puffing up* the middle of the LF and causing the fitting process to find an artificially high α as the IMF tries to produce more single WDs of intermediate age. The error in the fitting process is understandably higher in this case because it becomes difficult to fit the LF with a single power-law IMF. When we include the 40% binary fraction in the initial population, its nondynamical PDMF at 4 Gyr is best fitted with $\alpha = 3.15$ (0.48). After 1 Gyr the LF for all cluster WDs, including double WDs, is best fitted by $\alpha = 2.75$ (0.93), and after 2 Gyr it is best fitted by $\alpha = 3.00$ (0.43). Thus, the LF for all WDs is affected by the cluster environment at a much earlier stage than for the standard single WDs, first indicating a flatter than expected mass function, which then becomes steeper than expected at later times.

5.2. Half-Mass Radius

In Figure 7 we break the LF for all WDs at 4 Gyr into two separate LFs depending on whether the WD is inside or outside the cluster half-mass radius. Performing a χ^2 test on the two LFs reveals a probability of 0.01 that they are drawn from the same distribution. The inferred IMF slope for $r < r_h$ is $\alpha = 3.90$ (0.86), and exterior to r_h it is $\alpha = 3.55$ (0.26), which makes sense on the basis of mass segregation increasing the proportion of double WDs and luminous single WDs in the central regions (see also Fig. 2d). Considering only the standard single WDs, the best fits are $\alpha = 3.30$ (0.94) for $r < r_h$ and $\alpha = 3.00$ (0.46) for $r > r_h$. The results of the LF fits at 1, 2, and 4 Gyr for the simulations starting with $N = 28,000$ and $f_b = 40\%$ are summarized in Table 1.
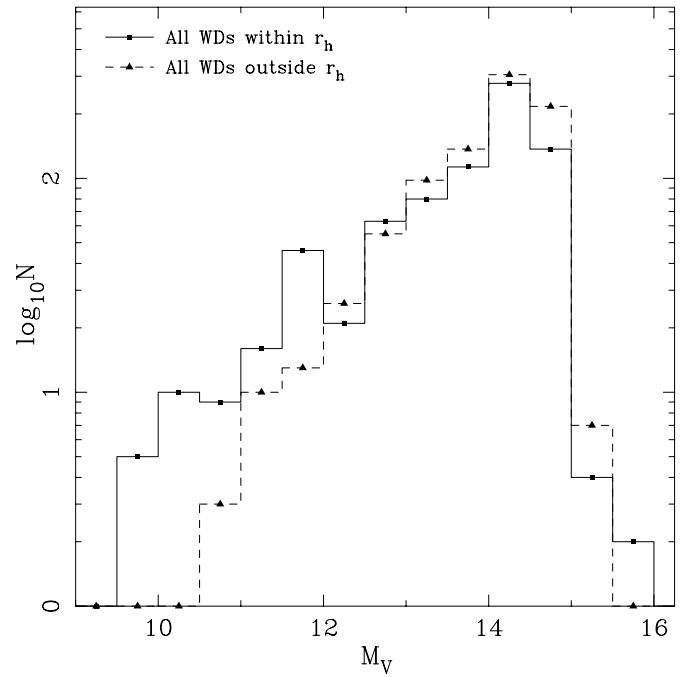

Fig. 7.—WD luminosity functions at 4 Gyr for all WDs interior (*solid line*) and exterior (*dashed line*) to the cluster half-mass radius. The best-fitting Salpeter (1955) IMFs for each case have slopes of $\alpha = 3.90$ and $\alpha = 3.55$, respectively.

It is clear from Figure 7 that the most luminous WDs are preferentially found interior to r_h. We find that when a WD appears at the top of the cooling track it is most likely to be found at a radial distance of $0.6 r_{h,\mathrm{WD}}$ from the cluster center, where $r_{h,\mathrm{WD}}$ is the half-mass radius of the WDs, which is itself less than r_h (for $t < 5$ Gyr). Then, as the WD cools it will relax out to $r_{h,\mathrm{WD}}$ on a timescale equivalent to twice the current half-mass relaxation timescale. By the time the WD reaches the bottom of the cooling track it will have relaxed even further to blend in with the spatial distribution of the cool WDs. As the cluster evolves, the fraction of luminous WDs found interior to r_h decreases. Defining a luminous WD as one appearing in the upper 4 mag of the WD sequence ($M_V < 14$ at 4 Gyr), we find that 19% of the standard WDs with $r < r_h$ at 4 Gyr are luminous whereas 40% are luminous at 1 Gyr. Exterior to r_h the numbers are 14% and 24%, which means that over time the difference between the two populations is also decreasing. This is apparent in Table 1, where we see that the difference between the LFs for WDs interior and exterior to r_h, in terms of the α fitted to each LF, decreases as the cluster ages.

TABLE 1
LUMINOSITY FUNCTION DATA FOR SIMULATIONS WITH $N = 28,000$ AND $f_b = 40\%$

AGE (Gyr)	ALL WDs		$r < r_h$		$r > r_h$		STANDARD SINGLE WDs		$r < r_h$		$r > r_h$	
	α	Probability	α	Probability	α	Probability	α	Probability	α	Probability	α	Probability
1.0.......	2.75	0.93	3.55	0.24	2.40	0.28	2.70	0.87	3.15	0.89	2.15	0.31
2.0.......	3.00	0.43	3.65	0.16	2.75	0.65	2.80	0.76	3.20	0.85	2.65	0.97
4.0.......	3.75	0.30	3.90	0.86	3.55	0.26	3.15	0.65	3.30	0.94	3.00	0.46

NOTE.—The results of the fitting process are given for LFs containing all WDs, including double WDs, and those containing only the WDs identified as being standard single. We consider LFs for the entire cluster and also for WDs interior or exterior to the cluster half-mass radius. In each case we give the best-fitting α from a single power-law Salpeter 1955 IMF, based on the minimum χ^2, and the probability that this provides a good fit to the data.

5.3. *Exchanges and Escapers*

The reason for the steepening with time of the IMF inferred from the standard single-WD population of the cluster is not an overabundance of luminous WDs but rather the preferential escape of older less luminous WDs from the cluster because these are more likely to reside in the outer regions. We recall from the previous section that the fraction of escaping WDs increases as the cluster evolves. Strong dynamical interactions with other cluster stars also alter the makeup of the standard single-WD population, but here the effect on the LF is less clear. After 4 Gyr 14% of the potential standard single WDs have been lost from the population because they, or their MS star or giant precursors, have been exchanged into binary systems.[5] This accounts for 49% of the total number of exchange interactions recorded in the 4 Gyr of cluster evolution. In raw numbers this amounts to a loss of 140 potential standard single WDs: 19 of these were exchanged into a binary after becoming a WD, and 12 of the double WDs present at 4 Gyr contain a WD that would have been a standard single WD without dynamical intervention. At any point in time this process is more likely to affect luminous WDs because these reside in higher density regions, but over the lifetime of the cluster both cool and hot WDs are affected and the change to the LF slope is minimal. After 1 Gyr of cluster evolution 6% of the standard single-WD population has been lost owing to exchange interactions (8% after 2 Gyr), accounting for 24% of all exchanges to that point (37% after 2 Gyr), and none are found in double WDs. Therefore, as the cluster evolves, the standard single WDs become involved in dynamical encounters to a greater degree, but the effect remains secondary to the escape of cool WDs in explaining the steepening of the inferred IMF.

An examination of all WDs appearing in the cluster WD sequence, including double WDs, shows that the LF at 1 Gyr has suffered from a decrease in the relative number counts at the bright end (as evidenced by the lower than expected α). There are a number of ways that the cluster environment could be producing this effect. The presence of wide double-WD binaries in the core leaves this population exposed to disruption by three- and four-body encounters. The presence in the core of binaries composed of a WD and a nuclear burning star that will soon evolve to become a WD raises the possibility of three-body interactions exchanging the WD for a slightly more massive MS star so this system will not reach the WD sequence. Furthermore, the progenitors of short-period double WDs, which are formed via a common-envelope phase, may be hardened by three-body encounters, and as a result the common envelope is formed earlier than expected, thus accelerating the formation of the double WD or even resulting in a merger event. The time at which the value of the IMF slope inferred from the LF of all WDs matches the expected nondynamical value ($\alpha = 3.15$) is ~ 2.4 Gyr. By this time the density of stars in the inner regions of the cluster was approximately a factor of 10 less than the starting value, making dynamical modification of the cluster populations less likely, and the escape of cool WDs had started to dominate in terms of shaping the LF.

5.4. *Where to Observe?*

Brocato et al. (1999) have already demonstrated that variations to the IMF do not alter the location of the LF maximum and therefore calculations of the cluster age using this method are not sensitive to errors in the IMF slope. However, for the more sophisticated method of fitting the entire LF (e.g., Hansen et al. 2002) the method *is* sensitive to the IMF because it alters the relative number of WDs in each luminosity (or mass) bin. Working on the premise that we are interested in deriving an age for a star cluster by fitting the WD LF and that we are going to consider only cooling models of standard single WDs in this process, then the question is this: where in the cluster should we look in order to extract the correct PDMF, i.e., an IMF slope of $\alpha = 2.7$ for the single WDs? The simple answer for our models at 4 Gyr is *nowhere*. At this point the cluster is dynamically well evolved (12 half-mass relaxation timescales have elapsed) and the cluster environment has effectively removed all trace of the IMF from the WD population. The region where we come closest to recovering the PDMF is $1 < r/r_h < 2$, where $\alpha = 2.95$ for the standard single WDs. At earlier times the situation is not so severe. After 1 Gyr (three half-mass relaxation timescales) and 2 Gyr (five half-mass relaxation timescales) the PDMF for single WDs is recovered by considering only standard single WDs in the region $0.5 < r/r_h < 1.0$. Owing to the fact that the WDs are centrally concentrated with respect to nuclear burning single stars at these times (see top panels of Fig. 5), it is understandable that we need to look inside r_h to find the PDMF. Outside r_h there is a paucity of massive stars and therefore a deficiency of young WDs, flattening the inferred IMF, and conversely we would expect an overabundance of young WDs in the very central regions of the cluster, slightly offset by the presence of the majority of the very massive old WDs. Thus, assuming that our observations are accurate enough that we can remove a substantial fraction of the double WDs from the LF, then using the LF of WDs residing in the $0.5 < r/r_h < 1.0$ portion of a young cluster should provide a reliable age (although the nonstandard single WDs still remain; see § 7.1). If double WDs cannot be removed, then binary evolution, as well as dynamical effects, must be accounted for in the fitting process. Factors such as the relative fraction of DA to DB WDs also play a role in determining the shape of the LF (Hansen et al. 2002).

5.5. *Metallicity*

The metallicity of the cluster population influences the LF fitting process in a number of ways. First, the upper mass limit for a ZAMS star that will evolve to produce a WD has been shown to vary with Z: it decreases from 8.0 $M_\odot$ for $Z = 0.02$ to 6.8 $M_\odot$ for $Z = 0.0001$ in our adopted stellar evolution algorithm. This mass limit is found by inspecting detailed stellar models to determine at what mass carbon ignites in the core of an asymptotic giant branch (AGB) star, and the subsequent burning of this carbon produces an ONe core larger than the Chandrasekhar mass (Pols et al. 1998). The actual upper mass limit may be slightly less than this depending on the mass-loss rate assumed for stars on the AGB.[6] Second, the mass of a WD

---

[5] The approximate timescale (Davies 1995) for a 1.4 $M_\odot$ MS star to be exchanged into a binary consisting of 1.0 and 0.5 $M_\odot$ MS stars is 1 Gyr if the binary is in the core of the cluster and has a semimajor axis of 10 AU (or equivalently if the binary is at r_h and has a semimajor axis of 50 AU).

[6] Hurley et al. (2000) provide a description of the mass-loss rate used in the stellar evolution algorithm and also a more complete description of the WD upper mass limit.

at birth depends on competition between the rate of growth of the degenerate core of its AGB star progenitor and the rate at which the envelope of the star is depleted by mass loss—both of which depend to some degree on Z. Finally, the lifetime of an MS star depends on its initial composition, shortening with decreasing metallicity for the range of initial masses that produce WDs. For example, the MS lifetime of a 2 $M_\odot$ star decreases by $\sim 60\%$ when the metallicity of the star is reduced from $Z = 0.02$ to 0.0001. This has the effect of lowering the MS turnoff mass for low-metallicity clusters and increasing the age of the WDs relative to MS stars. All of these effects are naturally accounted for in the LF fitting process provided that the correct metallicity is used when the theoretical LF is generated. Of the four N-body simulations described by Shara & Hurley (2002), each starting with $N = 20,000$ and $f_b = 10\%$, two were performed with $Z = 0.004$ while the other two had solar metallicity. We find that regardless of metallicity, the LFs for the standard single WDs at 4 Gyr in each of these simulations are best fitted by an IMF slope of $\alpha \simeq 3.05$, noting that the range of ZAMS masses producing WDs at this time for $Z = 0.004$ is 1.2–7.0 $M_\odot$. We also find that metallicity has a negligible effect on the WD mass fraction of a cluster (see next section), in agreement with von Hippel (1998).

6. THE CLUSTER WHITE DWARF MASS FRACTION

Figure 8 shows the fraction of the cluster mass contained in WDs as a function of time for the N-body simulations with $N = 28,000$ and $f_b = 40\%$ discussed in this paper. Also
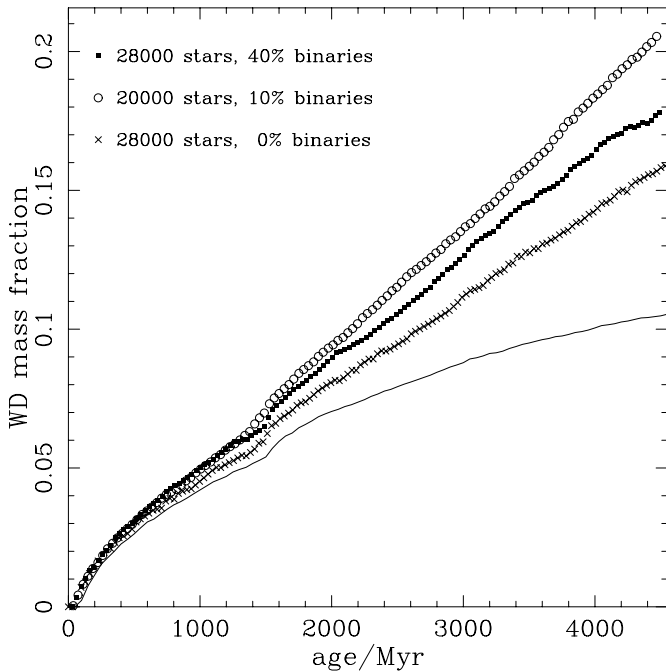

FIG. 8.—WD mass fraction as a function of cluster age for simulations with 28,000 stars and a 40% binary fraction (*filled squares*), 20,000 stars and a 10% binary fraction (*open circles*), and 28,000 with no primordial binaries (*crosses*). The corresponding mass fractions for the same populations evolved outside of the N-body code are also shown (*solid line*). Note that the mass fractions have been normalized so that the nondynamical populations produce the same mass fraction of WDs (although the difference at any particular time is never more than a few percent). The remarkable deficit in WD mass fraction at 40% binaries relative to 10% binaries is discussed in § 6.

shown is the WD mass fraction, f_{WD}, for the same primordial populations evolved without dynamics. It is clear that as time progresses and the simulated clusters become dynamically more evolved, the cluster environment has a significant effect on the measured WD mass fraction. More correctly, it is a combination of the cluster environment and the environment that the cluster resides in that is producing this effect; i.e., mass segregation causes low-mass MS stars to move to the outer regions of the cluster so these stars are preferentially stripped from the cluster relative to heavier objects such as WDs (see § 4). Therefore, even though properties of the WD population such as its total mass are relatively unaffected by the dynamical evolution of the cluster, the WD mass fraction is affected and all clusters will become rich in WDs in the late stages of their evolution (see also Vesperini & Heggie 1997; Portegies Zwart et al. 2001).

For young open clusters, less than ~ 3–4 relaxation times old, the results of our simulations suggest that it is safe to assume that the WD mass fraction has been little affected by the kinematic evolution of the cluster (von Hippel 1998). However, for older open clusters and for globular clusters it would be incorrect to make this assumption. Vesperini & Heggie (1997) used N-body models with $N = 4096$ stars to investigate f_{WD} after 15 Gyr of evolution for globular clusters born with $N \sim 10^5$ stars. For a cluster orbiting within the Galactic potential at a distance of 4 kpc from the Galactic center they found $f_{WD} = 0.277$ (with some dependence on the IMF and density profile chosen for the model). Checking their results by performing additional simulations of $N = 8192$ and $N = 16,384$ stars, they found $f_{WD} = 0.345$ and $f_{WD} = 0.422$, respectively. This lack of convergence for increasing N demonstrates the perils of scaling the results of small-N simulations to large-N clusters. However, owing to the difficulty in performing direct N-body models of globular clusters, scaling is often unavoidable, and in that case our value of $f_{WD} \simeq 0.18$ at 4 Gyr may be taken as a lower limit of the true value for an old globular cluster.

Vesperini & Heggie (1997) showed that the position of a star cluster in the Galaxy is a factor in determining its WD mass fraction. They found that clusters orbiting at 4 kpc have f_{WD} increased by more than a factor of 2 over clusters at 16 kpc. Therefore, we would expect globular clusters such as M4, which has a perigalacticon of 1 kpc (Peterson, Rees, & Cudworth 1995), to exhibit dynamically enhanced WD mass fractions. For M4 this is supported by observations showing that its MF for stars less massive than 0.65 $M_\odot$ has a slope of only $\alpha = 0.75$ (Richer et al. 2002). In light of these results it would seem that the assumption by von Hippel (1998) that the WD mass fraction of M4 has not been affected by the kinematic evolution of the cluster is in error. *We urge anyone utilizing observations of the WD mass fraction in dynamically evolved star clusters, and especially those clusters orbiting near the Galactic center, to account for the dynamical history of the cluster.* We note that the position in our simulated clusters where f_{WD} matches that of the nondynamical population, after 4 Gyr, is at three half-mass radii from the cluster center.

After 4 Gyr of cluster evolution, or ~ 12 half-mass relaxation times, f_{WD} has approximately doubled in comparison to the same population evolved without dynamics. This translates to an error of $\Delta\alpha \simeq 0.2$, or 10%, in the slope of the inferred power-law IMF if the dynamical evolution is ignored. Portegies Zwart et al. (2001) demonstrated that the dynamical evolution of a cluster has little effect on the

numbers of giants and WDs present in the population and therefore that the relative number of these stars may be used to constrain the IMF of a star cluster. However, in making this point Portegies Zwart et al. (2001) were only drawing upon the results of small-N simulations at 0.6 Gyr (after $\sim$6 relaxation times). Our simulations with $N = 28,000$ and $f_b = 40\%$ also show minimal modification of the giant and WD numbers for the same degree of dynamical evolution ($\sim$2 Gyr for our larger N), but after 4 Gyr this is no longer true: only 48% of the expected number of giants, and 50% of the expected number of WDs, are present in the cluster at this time. Remarkably, the number ratio of the two populations is still intact and would provide a reliable estimate of the IMF. Depletion of the number of WDs is primarily the result of WDs escaping from the cluster—this accounts for 80% of the decrease—with the remainder of the depletion explained by enhanced binary interaction. Giants are much less likely to escape from the cluster because their lifetimes are extremely short compared to MS and WD lifetimes. As such, only 4% of the expected population of giants at 4 Gyr was lost as a result of giants escaping the cluster. An additional 20% of the expected giants were lost as a result of MS stars that would have evolved to appear as cluster giants at 4 Gyr escaping prior to this time. The remaining 23%, i.e., $\sim$50% of the decrease, is explained by the depletion of giants, or their MS progenitors, in three- and four-body encounters.

In Figure 8 we also show the evolution of $f_{\rm WD}$ with time for simulations with $N = 20,000$ and $f_b = 10\%$ and for simulations with $N = 28,000$ and no primordial binaries. We believe that the difference in $f_{\rm WD}$ between the two different families of N-body simulations with primordial binaries is real and can be explained in terms of binary fraction, and to a lesser extent the initial period distribution assumed for the binaries. Consider that a noninteracting, i.e., wide, binary composed of two 2.0 $M_\odot$ stars will evolve to contribute two $\sim$0.65 $M_\odot$ WDs to the cluster WD population. If instead the binary components do interact and merge to form a single star (initial periods less than $\sim$2200 days), then only one WD with a mass in the range $\sim$0.8–0.9 $M_\odot$, depending on the binary period, will be contributed. Therefore, the evolution of close binaries can decrease the mass in WDs. As a result, the simulations with a large binary fraction (40%) experience a larger relative decrease in the WD mass fraction owing to binary evolution than those with a moderate binary fraction (10%). A larger binary fraction also provides more scope for the cluster to increase the fraction of close binaries through three- and four-body encounters.

Comparisons between the simulations with and without primordial binaries simply using the cluster age can be misleading because the latter are dynamically less evolved at an age of 4 Gyr. Without binaries the half-mass relaxation timescale at 4 Gyr is $\sim$430 Myr, which is twice as long as the

timescale found for both families of simulations with primordial binaries. The primary reason for the difference is that clusters with a significant primordial binary population suffer a higher rate of mass loss from the cluster: 40% of the initial cluster mass remains at 4 Gyr for the $f_b = 0\%$ clusters, 27% for $f_b = 10\%$, and 21% for $f_b = 40\%$. An enhanced rate of escaping stars via velocity kicks obtained in three-body interactions is the explanation for this trend. If we instead make a comparison of $f_{\rm WD}$ when the simulated clusters are all at the same dynamical age (10 half-mass relaxation timescales old), then we find 0.168 for $f_b = 0\%$ (4730 Myr), 0.170 for $f_b = 10\%$ (3720 Myr), and 0.147 for $f_b = 40\%$ (3510 Myr).

7. DISCUSSION AND FURTHER ANALYSIS

Using the results of N-body simulations to investigate and understand the nature of WD populations in star clusters, in terms of appearance in the CMD, the luminosity function, and mass fraction, appears to be a worthwhile approach. However, to this point we have concentrated on one particular type of simulation with its unique set of initial conditions. Variations to the model parameters, which range from the initial setup of the cluster to aspects of binary evolution, have the capability to influence the results. Here we discuss which parameters are of greatest importance and look at how our results can be utilized to interpret observations of WD populations in star clusters.

7.1. Variation of Cluster Parameters

We have already seen in § 6 that the primordial binary fraction of a star cluster plays a role in determining the evolutionary characteristics of the cluster, such as the escape rate of the stars and the relaxation timescale, as well as affecting aspects of the stellar populations, namely, the WD mass fraction. Similarly, we would expect the binary fraction to have an impact on the shape of the WD luminosity function and the appearance of the WD sequence in the CMD. In Tables 2 and 3 we have replicated the luminosity function results of Table 1 but this time for the simulations with $f_b = 10\%$ and $f_b = 0\%$, respectively. For $f_b = 10\%$ the trends in the LF data are similar to those found for the simulations with $f_b = 40\%$, but in general the behavior is less extreme. As an example, the LF for standard single WDs at 4 Gyr is best fitted by $\alpha = 3.05$, as opposed to $\alpha = 3.15$ for $f_b = 40\%$, so it is closer to the nondynamical expected value. The probability of the fit being a good one is also higher, which is an indication of a lower degree of contamination in the WD sequence. The reason for this is most likely a combination of the $f_b = 10\%$ clusters having lost less of their stars at the same age and the fact that a smaller fraction of standard single WDs have been affected by dynamical

TABLE 2
LUMINOSITY FUNCTION DATA FOR SIMULATIONS WITH $N = 20,000$ AND $f_b = 10\%$

AGE (Gyr)	ALL WDs		$r < r_h$		$r > r_h$		STANDARD SINGLE WDs		$r < r_h$		$r > r_h$	
	α	Probability	α	Probability	α	Probability	α	Probability	α	Probability	α	Probability
1.0.......	2.70	0.92	3.30	0.69	2.00	0.10	2.70	0.88	2.90	0.89	2.00	0.08
2.0.......	3.20	0.35	3.45	0.07	2.35	0.40	2.75	0.26	3.20	0.06	2.25	0.68
4.0.......	3.40	0.62	3.55	0.77	3.25	0.83	3.05	0.82	3.30	0.93	3.00	0.93

TABLE 3
Luminosity Function Data for Simulations with $N = 28,000$ and $f_b = 0\%$

Age (Gyr)	All WDs		$r < r_h$		$r > r_h$		Standard Single WDs		$r < r_h$		$r > r_h$	
	α	Probability	α	Probability	α	Probability	α	Probability	α	Probability	α	Probability
1.0.......	2.70	0.97	2.95	0.88	2.15	0.47	2.70	0.97	2.95	0.88	2.15	0.47
2.0.......	2.80	0.89	2.95	0.83	2.05	0.99	2.80	0.90	2.95	0.82	2.05	0.99
4.0.......	3.05	0.66	3.15	0.90	3.05	0.80	3.05	0.67	3.15	0.91	3.05	0.79

interactions. We note that the clusters with only 10% primordial binaries have a smaller total number of stars than those with 40% primordial binaries. This may also be a factor in any differences between the two types of simulation, but on the other hand the total number of systems, single stars and binaries, is equal.

For the simulations without primordial binaries the first binary formed after ~300 Myr of evolution, which is roughly the half-mass relaxation timescale at that time. The number of binaries in the simulation jumps sharply at the time of core collapse (~1400 Myr, or ~3 half-mass relaxation times), but even so, the number is only seven, or 0.03%. The binary frequency subsequently reaches a peak of 0.07% after ~3500 Myr and basically stays at this value for the remainder of the simulation. Owing to the lack of binaries in these simulations, it is not surprising to see minimal contamination of the WD LF by double WDs and nonstandard single WDs—the LF results in Table 3 for all WDs and standard single WDs are identical. However, the shape of the WD LF has still been affected by the dynamical evolution of the cluster, and the behavior is similar to that found for the $f_b = 10\%$ simulations.

We note that for all of the LF fits described in Tables 1, 2, and 3 the value of the χ^2 statistic for the fit is less than that given by the $\sqrt{N}$ uncertainty in the data points, except in two cases—the $r > r_h$ fits for all WDs and standard single WDs at 1 Gyr for the $f_b = 10\%$ simulations. Both LFs suffered from a distinct lack of hot WDs for $M_V < 13$, which meant that only four data points were available to be fitted.

In § 5.4 we found that after 1 and 2 Gyr of cluster evolution the best place to look for the true nondynamical PDMF of the standard single WDs was in the region $0.5 < r/r_h < 1.0$, in the case of the $f_b = 40\%$ simulations. This is also true for the other simulations that we have considered, although for $f_b = 0\%$ at 1 Gyr it is best to look closer to $0.5r_h$, and for both $f_b = 0\%$ and $f_b = 10\%$ clusters at 2 Gyr it is best to look closer to r_h. For all the simulation types it is not possible to recover the PDMF after 4 Gyr of evolution.

An interesting question is whether we can quantify our findings on the contamination of the WD sequence in such a way as to help observers of open clusters produce clean WD LFs. As shown in Table 4 the level of contamination clearly increases with an increasing cluster primordial binary fraction, in terms of both the number of nonstandard single WDs and double WDs produced and the dynamical removal of standard single WDs. We have also included in Table 4 the ratio of double WDs to single WDs, and the ratio of nonstandard single WDs to all single WDs, for the three distinct types of simulation. Unfortunately, there is no clear relation between these two numbers, except that as one increases so does the other. One or two more data points and more simulations to decrease the noise in these results may lead to a more promising result. In the meantime, the numbers presented in Table 4 should prove useful, especially if observations are good enough to separate the majority of double WDs from the single-WD sequence in the CMD and therefore gain an accurate estimate of the ratio of double WDs to single WDs. Alternatively, the binary fraction of the cluster, or at least a lower limit, may be known from observations of the main sequence (e.g., Montgomery, Marschall, & Janes 1993). Either way, the results of our simulations can then be used to estimate what fraction of nonstandard single WDs are present and remove these from the LF, although the behavior of this fraction with magnitude is required for this approach to be of most use. Our recommendation for anyone wishing to derive information from the WD LF of a dynamically evolved star cluster is that they request data for simulations that best match the parameters of the observed cluster (age, binary fraction, etc.).

Any aspect of the initial conditions chosen for a particular simulation that has the potential to affect the lifetime of the cluster or the amount of dynamical activity also has the

TABLE 4
Contamination of the WD Sequence at 4 Gyr for the Various Simulation Classes

Simulation (1)	n_{nss} (2)	n_{DWD} (3)	$n_{ss,ex}$ (4)	$n_{ss,ex}/n_{ex}$ (5)	n_{DWD}/n_s (6)	n_{nss}/n_s (7)
$N = 28,000, f_b = 40\%$.....	694	230	162	0.49	0.136	0.410
$N = 20,000, f_b = 10\%$.....	213	36	109	0.61	0.030	0.176
$N = 28,000, f_b = 0\%$	8	4	42	0.62	0.004	0.008

Note.—Col. (1): Type of simulation. Cols. (2) and (3): Number of nonstandard single WDs (n_{nss}) and number of double WDs (n_{DWD}) in the WD sequence. Col. (4): Number of expected standard single WDs (n_{ss}) that are exchanged into binary systems. Col. (5): Fraction of all exchange interactions that this comprises. Note that the numbers in Cols. (2), (3), and (4) are per 1000 standard single WDs. Cols. (6) and (7): ratio of nonstandard single WDs and double WDs, respectively, to the total number of single WDs ($n_s = n_{ss} + n_{nss}$).

potential to alter the makeup of the resultant stellar populations and therefore create uncertainty in our results. In addition to binary fraction the parameters that immediately spring to mind are the number of stars, the density profile, and the external potential in which the cluster will orbit. Indeed, Vesperini & Heggie (1997) have shown that both the shape of the cluster mass function and the WD mass fraction are significantly affected by the starting value of N and the position of the cluster in the Galaxy, while the choice of initial density profile is less important. However, these results are only for models of single stars, and it is the lack of large-scale simulations with substantial binary populations and a realistic treatment of binary evolution that makes it difficult to quantify the broader impact of these parameters on the stellar populations of clusters. This is precisely what we have started to address in the work presented here, but considering that each of our $f_b = 40\%$ simulations took a minimum of 4 weeks to perform, a full parameter study will take time. To investigate the actual behavior of the WD population in a globular cluster we need to push the particle number of our simulations to at least 10^5, and recently Baumgardt & Makino (2003) have taken steps in this direction. With a single GRAPE-6 board and a primordial binary fraction of only a few percent, it is estimated that a full-scale simulation with $N = 10^5$ will take a minimum of 4 months to evolve to 10 Gyr.

7.2. *Variation of Stellar and Binary Evolution Parameters*

In the NBODY4 code all aspects of standard binary evolution, i.e., nonperturbed orbits, are treated according to the prescription described in Hurley, Tout, & Pols (2002). The problem with modeling binary evolution, whether it be by a prescription-based approach or using a detailed evolution code (Nelson & Eggleton 2001), is that the outcome is extremely dependent on the input parameters to the model, which are themselves uncertain. Furthermore, we are not even sure of how to model some of the processes that arise. Take, for example, common-envelope evolution, which is assumed to occur when mass transfer becomes unstable. In this case a detailed model of the process is still beyond us, and those working in the field of binary population synthesis cannot even agree on a standard form for a simple model (Iben & Livio 1993; Nelemans et al. 2001; Hurley et al. 2002), let alone parameters of the model such as the common-envelope efficiency parameter, α_{CE}. The uncertainty that this creates is substantial because in population synthesis the common-envelope phase is crucial for the production of binaries such as cataclysmic variables and short-period double WDs. For the N-body simulations described in this paper we have used $\alpha_{CE} = 3.0$ because this was shown by Hurley et al. (2002) to give good agreement with observationally determined Galactic formation rates of various binary populations, although in most cases the observational tests were not particularly stringent. For example, Hurley et al. (2002) showed that using $\alpha_{CE} = 1.0$ does not predict enough short-period (<10 days) double WDs, compared to local observations, whereas $\alpha_{CE} = 3.0$ does. Hurley et al. (2002) investigated the influence of a number of model parameters on the predicted Galactic formation rate of double WDs. They found that the rate was not particularly sensitive to the choice of model for tidal evolution of the binary system, the metallicity of the population, or the initial eccentricity distribution and changed only marginally with variation in

TABLE 5
RESULTS FOR POPULATION SYNTHESIS MODELS AT AN AGE OF 4 Gyr

Model (1)	f_{DWD} (2)	α (3)	Probability (4)	Probability (5)
STD...........	0.09	3.15	0.48	...
CE1............	0.07	3.15	0.75	0.98
IMF...........	0.01	2.55	0.99	0.00
SEP............	0.06	2.90	0.88	0.09

NOTE.—Col. (1): Model name (see text for details). Col. (2): Fraction of double-WD binaries present in the model. Col. (3): Best-fitting α from a single power-law Salpeter 1955 IMF, based on the minimum χ^2, to the WD LF. Col. (4): Probability that this provides a good fit to the data. Col. (5): Probability that the WD LF of the model and that of the STD model are drawn from the same distribution.

α_{CE} (within reasonable bounds of course). However, the predicted rate decreased by more than an order of magnitude when the component masses of each binary were drawn independently from the same IMF as opposed to assuming a uniform distribution for the mass ratios of the binaries, $n(q)$. These findings were in agreement with the extensive study of double-WD formation rates performed by Han (1998), using a different binary evolution model. In addition, Han (1998) considered the existence of a stellar wind, the velocity of this wind, enhancement of the stellar wind by the presence of a close companion, and the mass transfer efficiency of stable Roche lobe overflow as variable parameters and found that none of these had a substantial impact on the predicted rates.

In Table 5 we list population synthesis results relating to double WDs for the parameters of the binary population that we feel have the potential to change the outcome of our N-body simulations: α_{CE}, $n(q)$, and the initial distribution of the binary periods (or separations). The standard model (STD) assumes the parameters used in the N-body simulations, namely, $\alpha_{CE} = 3.0$, $n(q) = 1$, and the lognormal distribution of orbital separations given by Eggleton et al. (1989). In turn we then try models with $\alpha_{CE} = 1.0$ (CE1), binary component masses drawn independently from the IMF (IMF), and orbital separations chosen from a uniform distribution in the natural logarithm of the separation (SEP). Shown in Table 5 are the fraction of binaries that are double WDs and the value of α returned by fitting the WD LF (with corresponding probability of goodness of fit) after 4 Gyr. We also show the results of χ^2 tests between the WD LF of each model and that of the standard model. Clearly, the choice of $n(q)$ is the most crucial because the IMF model biases binaries to having small mass ratios and leads to a greatly reduced number of double WDs. The random pairing of binary component masses from the IMF is not well supported by observations (Eggleton et al. 1989; Duquennoy & Mayor 1991); however, Kroupa (1995) has shown that this assumption may be valid if most stars are formed in embedded star clusters. Furthermore, Tout (1991) has shown how selection effects make it difficult to determine $n(q)$ from observations. The distribution of orbital separations assumed in the SEP model is also not well supported by observations (Eggleton et al. 1989; Duquennoy & Mayor 1991), but once again the observed data is poorly constrained. It is comforting to see that the choice of α_{CE} has only a small effect on the number of double WDs in the model and that the appearance of the WD LF is unaffected, at least in the absence of dynamical interactions.

When considering the implications of the various models for the results of our N-body study we must also look at the distribution of orbital periods for the double-WD populations of each model. This will help to determine how potential modification of the double-WD population via interaction with the cluster environment may be affected. Figure 9a compares the distribution of double-WD periods at 4 Gyr arising from the STD model with that of the N-body simulations that started with $N = 28,000$ and $f_b = 40\%$. Thus, the initial conditions of the two models are identical, and the only difference is the presence of the cluster environment for

the latter. For the N-body simulations it is clear that dynamical interactions between the binary population and other cluster stars (or binaries) are effective in destroying the wide double-WD population, as expected, and in enhancing the number of close double WDs (as described by Shara & Hurley 2002). In Figure 9b we compare the STD and CE1 population synthesis models. The population of very wide double WDs is unaffected by the change in α_{CE} because their evolution did not involve a common-envelope event. Importantly, the relative number of double WDs in the intermediate-period range is reduced for $\alpha_{CE} = 1.0$, and it is
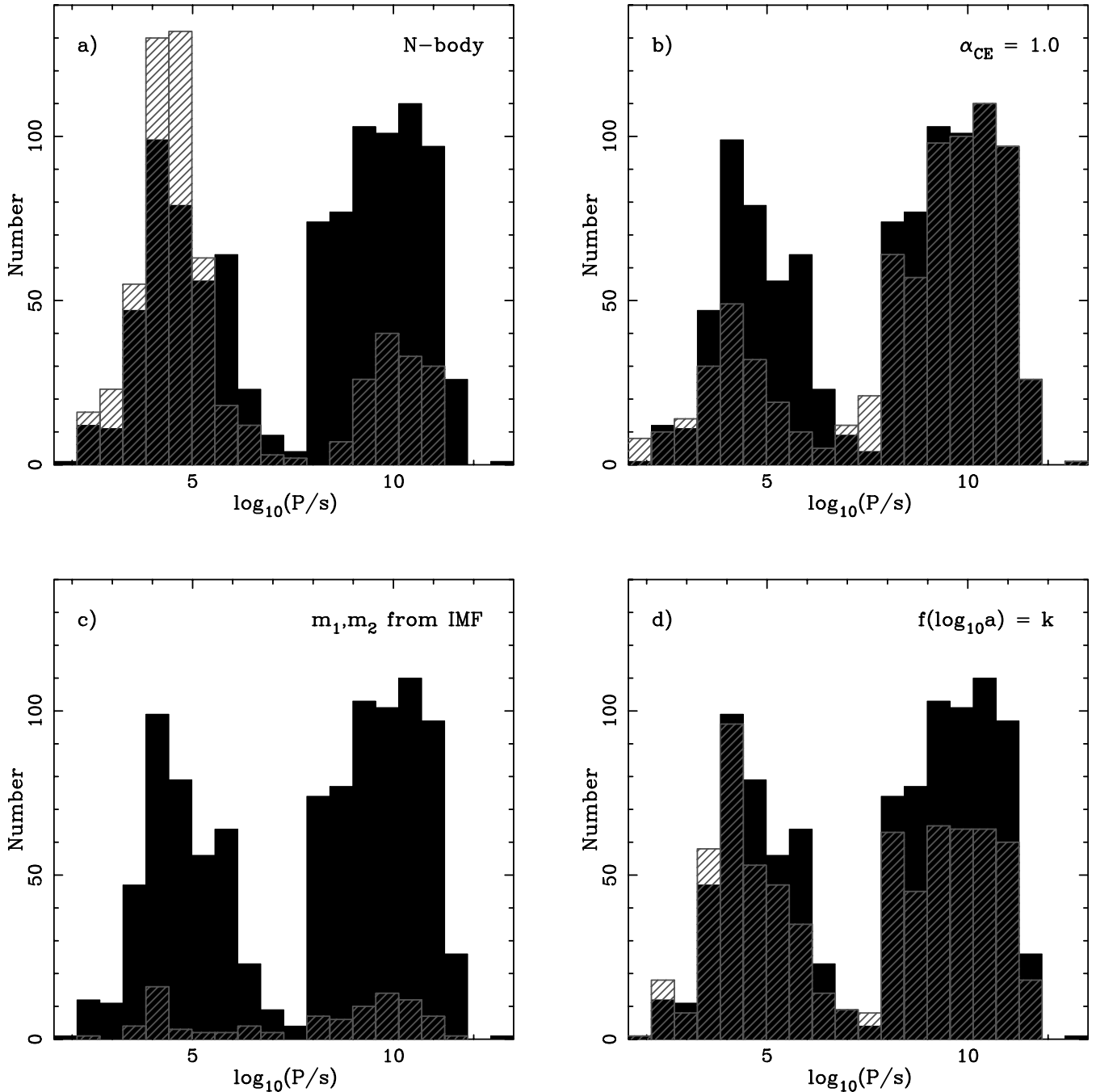

FIG. 9.—Distribution of orbital periods for double-WD populations at 4 Gyr of age. Panel (a) compares the distribution for the N-body simulations that started with 28,000 stars and a 40% binary fraction (*hatched histograms*) with the same population evolved outside the cluster environment (*solid histograms*; corresponds to population synthesis model STD). Panels (b), (c), and (d) compare the STD model (*solid histograms*) with the CE1, IMF, and SEP models, respectively (*hatched histograms in all cases*). [*See the electronic edition of the Journal for a color version of this figure.*]

this population that is most likely to be modified by the cluster environment and lead to an enhancement of short-period WDs. Therefore, our results are sensitive to changes in α_{CE}, with a lower α_{CE} leading to less contamination of the WD sequence by nonstandard single WDs. As expected, comparison of the STD and IMF models (see Fig. 9c) shows that the number of double WDs is greatly reduced across the entire period range when the binary component masses are randomly assigned, reinforcing that adoption of this initial condition would lead to substantially less interesting results regarding double WDs. The SEP model also shows a decrease in the number of intermediate-period double WDs (see Fig. 9d) but not to the same degree as seen in the CE1 model. The decrease in the number of wide double WDs is of little consequence for the N-body results.

The bottom line is that uncertainty in the parameters of binary evolution and the initial conditions of the binary population leads to uncertainty in the results of N-body simulations relating to binary populations. However, to explore the parameter space of binary evolution within the framework of N-body simulations would be an inefficient use of computational resources. What we can do is use the results of population synthesis calculations to determine which parameters are of greatest importance for future investigation. In the meantime, we can also hope that observational constraints on certain parameters will improve, as will our understanding of processes such as common-envelope evolution. What is beyond question is that the cluster environment is very effective in modifying the evolution of the binaries it contains.

The average WD mass of any stellar population depends to a large extent on the initial-final mass relation (IFMR), which links the ZAMS mass of a WD progenitor to the mass of the WD. The IFMR that results from the stellar evolution algorithm utilized in NBODY4 (Hurley et al. 2000) is biased toward higher WD masses, for ZAMS masses greater than ~ 3 $M_\odot$, than the semiempirical IFMR derived by Weidemann (1987) or the theoretical IFMR proposed by Han, Podsiadlowski, & Eggleton (1994, hereafter HPE). We note that the IFMR produced by the stellar evolution algorithm is not presupposed: it is a natural consequence of the combined effects of the mass-loss prescription adopted for AGB stars and the evolution of the core mass for AGB stars, as indicated by stellar models. It is also in good agreement with data on WDs observed in the young open cluster NGC 2516 (Jeffries 1997). After 4 Gyr of evolution for a nondynamical population of single stars drawn from the Kroupa et al. (1993) IMF, the average WD mass of the population is 0.66 if the SSE algorithm of Hurley et al. (2000) is used and 0.62 if the HPE IFMR is adopted, i.e., a difference of 6%. For the simulated clusters that started with 28,000 stars and $f_b = 40\%$ we found that the average WD mass and the average mass of the single MS stars reached equality after ~ 5050 Myr. If instead the HPE IFMR had been used, then the crossover would have occurred ~ 250 Myr earlier, i.e., a 5% error. An area where a change in the IFMR has the potential to make a noticeable difference is the WD mass fraction of the cluster, f_{WD}. However, for all of the N-body simulations we have presented, the value of f_{WD} that we estimate if we had instead used the HPE IFMR in the models is in good agreement with the results of § 6: for cluster ages in excess of 400 Myr it is always within 5% of the quoted values. Thus, all in all we do not expect a change in the IFMR to seriously alter our findings, especially at cluster ages

where the corresponding MS turnoff mass is below 3 $M_\odot$. One aspect that we have not considered in this analysis is that a decrease in the mass of a WD leads to an increase in its radius and therefore makes it more likely to interact with its companion if indeed the WD is a member of a binary. In the SSE algorithm a 4 $M_\odot$ ZAMS star would produce a ~ 0.8 $M_\odot$ WD, whereas use of the HPE IFMR would lead to a reduction of the WD mass by a factor of 7%, corresponding to an increase of 5% in the WD radius. To fully test the impact of this change on the results of our N-body simulations would require performing new simulations that adopted the HPE IFMR throughout. However, considering that agreement between the various IFMRs is quite good for ZAMS masses below 3 $M_\odot$ or cluster ages greater than ~ 500 Myr, we do not believe that this is a necessary course of action.

7.3. Comparison with Observed Data Sets

In recent years increased interest in the WD populations of star clusters, due in part to their potential use as stellar chronometers, has led to an increase in the available data relating to these populations (for recent reviews see von Hippel 1998; Koester 2002). The quality of these data sets has also improved but unfortunately not to the level where it allows rigorous comparison with our simulated clusters. Take, for example, the case of NGC 2420 (von Hippel & Gilmore 2000), where the use of *HST* has allowed the detection of eight WDs and the calculation of an age for the cluster largely independent of stellar models. This number of WDs is far too small to enable a meaningful statistical comparison with either the WD CMD or the WD LF of our models. On the other hand, observations of M67 (Richer et al. 1998) using the Canada-France-Hawaii Telescope have produced a much larger sample of WDs (of the order of 100), but problems of background contamination and the statistical subtraction of background sources persist. As a result, the WD LF is only a statistical representation of the true WD LF of the cluster, and it is not possible to identify the actual WD sequence in the CMD (as far as being sure that a particular point corresponds to a cluster member). Bearing in mind that the quality of the observed data sets will only improve in the near future, we shall persist and attempt some example comparisons using the existing data in order to demonstrate what may be gleaned from such an approach. Necessarily, we will focus on intermediate-age open clusters.

Richer et al. (1998) present a WD LF for M67 that after removal of background galaxies and field stars, and correction for incompleteness, contains 85 WDs down to the termination point of the cooling sequence. For comparison with the LFs of our N-body models at 4 Gyr, we have converted the observed LF to absolute magnitudes, using the distance modulus given by Richer et al. (1998), and normalized the simulated and observed LFs so that the peaks match in terms of magnitude and number. This required a shift of ~ 0.1 mag, which is representative of uncertainty in the cluster age: Richer et al. (1998) find a WD cooling age of 4.3 Gyr and an MS turnoff age of 4 Gyr. The normalization reveals that the observations are incomplete by a factor of ~ 20 in the next faintest magnitude bin after the peak and that the observed LF has too many hot WDs (by a factor of 4 for $M_V < 12.5$ bins), assuming that the simulated LFs are to be believed. Performing a χ^2 test with each of our three

distinct N-body data sets in turn shows that the observed LF is most likely drawn from the same population as the models with a 40% binary fraction (probability of 0.46)—a heartening result considering that Richer et al. (1998) quote a binary fraction of 50% for M67. Based on the number of giants present in the M67 CMD, Richer et al. (1998) estimate that they have found only 40% ± 10% of the expected number of WDs with cooling ages ≤1 Gyr. They also find that the mass fraction of WDs is 0.09, which is approximately half the number predicted by our 40% binary model at 4 Gyr, which itself is very similar to the observed parameters of M67. Therefore, we agree that M67 appears deficient

in hot WDs, indicating that dynamical interactions have been efficient in destroying hot WDs in this cluster.

The problems with foreground and background contamination that plague the interpretation of observations of open clusters such as M67 are not as severe in the case of the rich open cluster NGC 6819 (Kalirai et al. 2001c). Even though the photometry for NGC 6819 does not reach down to the termination of the WD sequence, the improved quality of the data (and better choice of filters) makes it possible to compare the upper part of the WD sequence with our cluster models. Figure 10a shows the potential WD candidates found in the CMD of NGC 6819 by Kalirai et al.
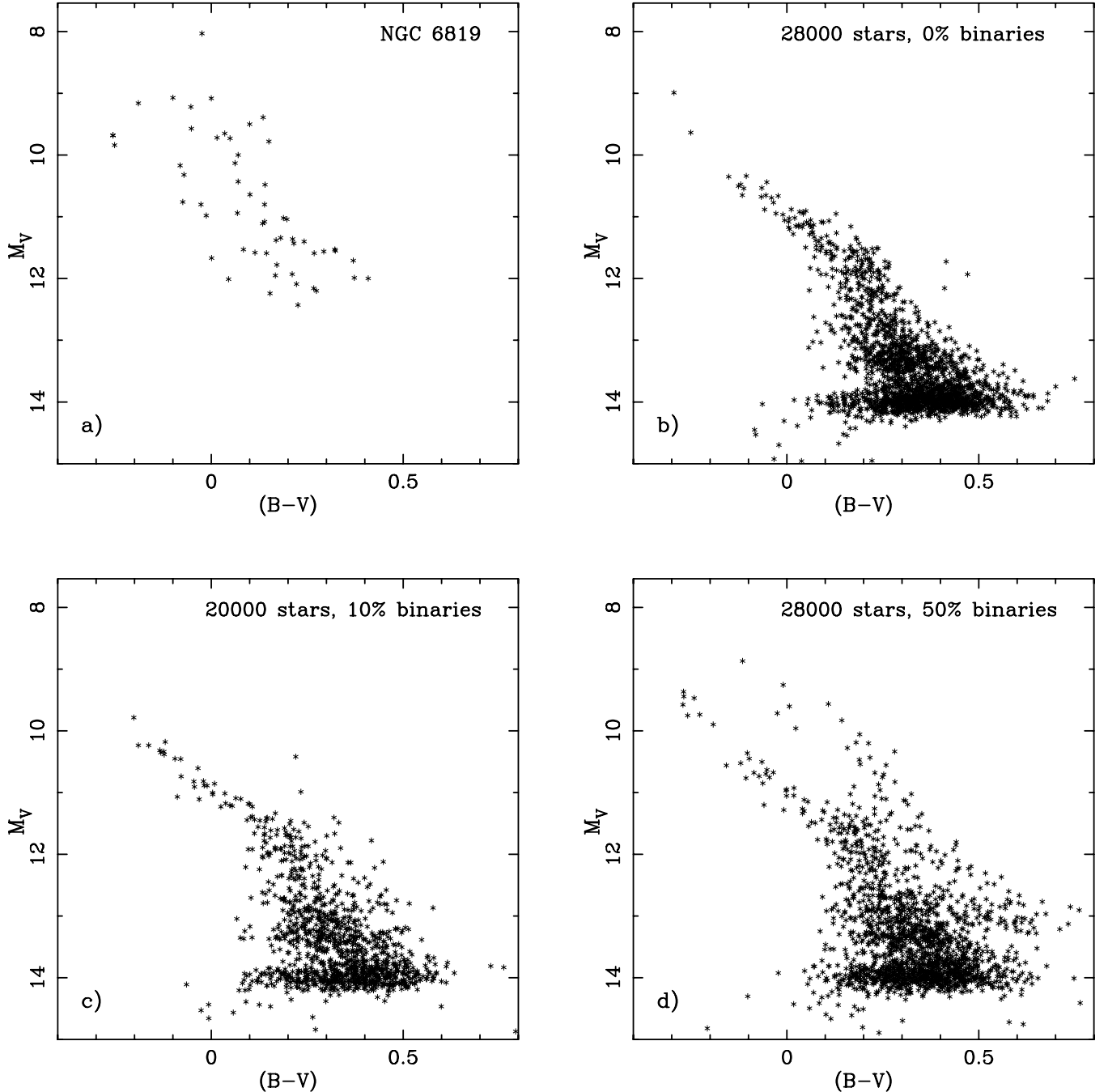

Fig. 10.—Cluster CMDs showing the WD sequence. (a) Observed data points for NGC 6819 after discarding objects with a stellarity index less than 0.75 (Kalirai et al. 2001c). (b, c, d) N-body models with 0%, 10%, and 40% primordial binaries, respectively, at an age of 2.5 Gyr. The N-body data has simulated photometric error added.

(2001c), including only objects that have stellarity index of 0.75 or greater (where 0 is most likely a galaxy and 1 is definitely a star). We note the existence of what appears to be two distinct WD sequences, where the brighter sequence is not consistent with being a population of background WDs with higher reddening nor can it be reproduced by a spread in WD masses (J. Kalirai 2002, private communication). The age of NGC 6819 is reported to be $\sim$2.5 Gyr (Rosvick & VandenBerg 1998; Kalirai et al. 2001c), so in Figures 10b, 10c, and 10d, we show the WD CMDs for our simulated clusters with 0%, 10%, and 50% binaries, respectively, at an age of 2.5 Gyr. For the sake of comparison we have added photometric error to the N-body data points in order to give an impression of how an observed WD sequence would appear (for a large open cluster) if all WDs were detected. The photometric error has been estimated using a rather simple expression that is basically Gaussian noise with a spread of $\pm A\sigma$ mag, where we have assumed $\sigma = 0.05$ in this instance. The value of A is given by $(m_x/10)^4$, where m_x is the magnitude of interest, and it is used to mimic the increasing error for decreasing brightness. A simple comparison by eye of the CMDs shown in Figure 10 indicates that the bright sequence of WDs in the NGC 6819 CMD could very well be the detection of a population of double WDs in the cluster and, if this is the case, that NGC 6819 most likely had a large fraction of primordial binaries. To aid the comparison we have merged Figures 10a and 10d with the result shown in Figure 11.

Although these two short examples have not led to any statistically significant conclusions, we maintain that they have served the purpose of demonstrating that comparisons of N-body models with observations of star clusters will lead to a better understanding of the nature of cluster WD populations. For open clusters we now have the tools in place to produce realistic model clusters that can be compared with
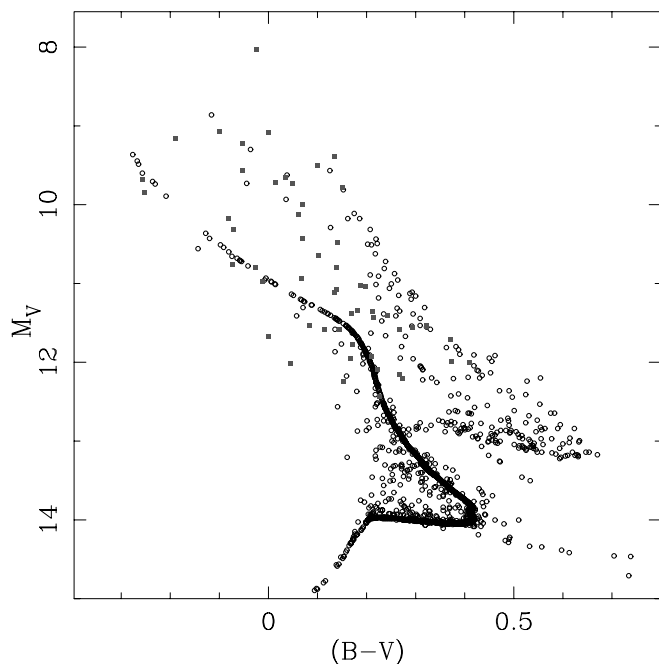
real clusters on a star-to-star basis. It will be particularly informative to tailor a set of simulations to an actual open cluster for which good-quality data exists, such as NGC 6819, with the initial conditions of the model hopefully constrained by observations. Such an approach will rely on close collaboration between stellar dynamicists and observers, and efforts in this direction are already underway.

Finally, we would like to comment on what our results can say about the excellent data set provided by HST observations of the globular cluster M4 (Richer et al. 2002; Hansen et al. 2002)—even though our N-body models fall far short of the particle number required for a globular cluster simulation. For M4 Hansen et al. (2002) used the method of fitting the entire WD LF to derive an age of 12.7 ± 0.7 Gyr for the cluster. In doing so they assumed an IMF slope of $\alpha = 1.05$, and they claim that the result is robust to changes in α as long as it remains in the range of 0.7–1.1. Their choice of α was based on a comparison of the number counts of WDs to low-mass MS stars in the cluster (Richer et al. 2002). Our simulations have shown that as a star cluster evolves, the value of the IMF slope inferred from the WD population steepens while the mass function of MS stars is flattened, primarily owing to stripping of stars from the cluster by the Galactic tidal field. M4 is not known to be a post–core-collapse cluster (Harris 1996), so it is not dynamically old, but its current half-mass relaxation timescale is estimated to be of the order of 500 Myr (Harris 1996). A conservative estimate of its dynamical age is probably in the range of 4–5 half-mass relaxation times old, considering that our N-body models have generally passed through core collapse by this point, and as such our results would predict that the WD LF should be well represented by a value of α only slightly greater than the IMF value. However, considering the orbit of M4 and the findings of Vesperini & Heggie (1997), we would expect the mass function of MS stars to have been significantly flattened at the low-mass end. Furthermore, Kroupa et al. (1993) have shown that for field stars the IMF slope for low-mass stars is considerably flatter ($\alpha = 1.3$ for $M < 0.5\ M_\odot$) than for stars in the WD-producing mass range. As a result, we find it surprising that the WD LF of M4 could be well fitted using such a low value of α. This could indicate that for M4 stellar interactions have been very effective in removing many of the hotter WDs (cf. the discussion of M67 above), an explanation that can also support arguments that the IMF of M4 was steeper than the PDMF quoted by Richer et al. (2002) while preserving the observed number counts. However, M4 is not a particularly dense globular cluster. Perhaps this is evidence that the IMF of M4 is different from that of field stars, but it is more likely that subtle effects, such as the stellar evolution age of M4 being much greater than our N-body models, led to differences in the evolution of the WD LF compared to our open cluster models.

8. SUMMARY

To first order, the WD population of a star cluster is relatively unaffected by the dynamical evolution of the cluster. However, segregation of the progenitor stars of the WDs, or binaries containing these progenitors, toward the center of the cluster and the stripping of low-mass stars by the Galactic tidal field affect both the appearance of the WD population and the WD mass fraction. In this work we have utilized the results of realistic N-body simulations of large

FIG. 11.—Same as Fig. 10 but with the NGC 6819 data (*filled squares*) combined with the WD sequence from the N-body models that started with 40% primordial binaries (*open circles*). [*See the electronic edition of the Journal for a color version of this figure.*]

open clusters to illustrate and quantify the behavior of WDs in dense star clusters.

We find that the presence of a substantial binary population in a star cluster, and the interaction of this population with the cluster environment, leads to a noticeable contamination of the observed WD sequence in the CMD by nonstandard single WDs and double-WD binaries. Scatter in the WD sequence produced by this contamination makes it difficult to judge the true bottom of the standard WD sequence, especially if a large population of old double WDs exists. This can lead to significant errors in the derived WD cooling age for the cluster. However, provided that the full extent of the WD sequence has been observed, the presence of nonstandard single WDs and double WDs in the WD LF does not affect the location of the LF peak. Thus, ages measured by this technique do *not* suffer any additional error. The shape of the LF *is* affected by the presence of nonstandard WDs, which produces an uncertainty in the inferred slope of the IMF. The amount of contamination of the WD LF by nonstandard single WDs is proportional to the number of double WDs in the cluster, which itself is linked to the primordial binary fraction of the cluster—if the number of double WDs observed in a real WD sequence is low, then it is safe to assume that the number of nonstandard single WDs is also low. Furthermore, the dynamical evolution of the cluster hampers the use of WDs as tracers of the IMF.

The results of our *N*-body simulations suggest that observations of star clusters should be conducted slightly interior to the half-mass radius of the cluster in order to best obtain information about the IMF from the WD LF. This region provides a compromise between our suggestion in § 3 that contamination of the WD sequence by double WDs is less of a problem exterior to r_h and our findings in § 5 that the true present-day mass function for single WDs is recovered for $0.5 < r/r_h < 1.0$, at least for clusters less than ~6 half-mass relaxation times old. For dynamically evolved star clusters the WD LF cannot be used to recover information about the slope of the IMF, regardless of the primordial binary fraction of the cluster. Our findings are particularly instructive for future *HST* observations of globular clusters where it is possible to observe only a portion of the cluster. Vesperini & Heggie (1997) have shown that for clusters that have undergone substantial dynamical evolution the PDMF for all cluster stars bears no relation to the IMF, even near the half-mass radius. This is especially true for globular clusters with orbits closer than 8 kpc to the Galactic center. Considering that large globular clusters are at an intermediate dynamical age and that the PDMF of MS stars loses memory of the IMF earlier than does the WD population, observations of the WD LF near the half-mass radius may be the best way to learn about the IMF of these objects. For open clusters it is generally possible to observe the entire cluster, at least for nearby clusters. In this case there is the

option to restrict the LF to include only WDs found in a certain region of the cluster. However, considering that open clusters contain fewer stars than globular clusters, this is a counterintuitive action in terms of obtaining a statistically significant result. Furthermore, open clusters are observed to have relatively high binary fractions (e.g., Richer et al. 1998), so contamination of the WD sequence by nonstandard single WDs and double WDs will be more of a problem. Therefore, we recommend that fitting of the WD LF for open clusters take into account the evolution of binaries and the cluster environment.

Our simulations have also shown that the WD mass fraction of a cluster is altered by the kinematic evolution of the cluster provided that it is more than a few relaxation times old. For a large open cluster after 4 Gyr of evolution, such as M67, the WD mass fraction is double the value expected from the same population evolved outside the cluster environment. This enhancement of the WD mass fraction is primarily explained by the preferential escape of low-mass stars from the cluster, and this result should be taken as a lower limit to the enhancement expected in moderate-size globular clusters. We find that enhancement of the WD mass fraction is not particularly sensitive to the primordial binary fraction of a star cluster. The expected number ratio of giants to WDs is preserved in our simulated clusters even though the two populations are affected in different ways by their residence in a cluster. Observation of this quantity is therefore one way to extract information about the IMF of an open cluster. Here, and in all instances, we must be very careful about scaling the results of our simulations to large-*N* globular clusters. Additional depletion of giants may be expected in the centers of globular clusters, which typically have much higher stellar densities than our models. Direct simulations of this type will be performed in the near future, providing additional information about the behavior of WDs, and all populations for that matter, in star clusters. Future models will also address the potential uncertainty in our results emanating from uncertainties in the parameters of binary evolution.

REFERENCES

Aarseth, S., Hénon, M., & Wielen, R. 1974, A&A, 37, 183
Aarseth, S. J. 1999, PASP, 111, 1333
Aarseth, S. J., & Heggie, D. C. 1998, MNRAS, 297, 794
Andreuzzi, G., Richer, H. B., Limongi, M., & Bolte, M. 2002, A&A, 390, 961
Baumgardt, H., & Makino, J. 2003, MNRAS, 340, 227
Benacquista, M. 1999, ApJ, 520, 233
Bergeron, P., Ruiz, M. T., & Leggett, S. K. 1997, ApJS, 108, 339
Bergeron, P., Wesemael, F., & Beauchamp, A. 1995, PASP, 107, 1047
Brocato, E., Castellani, V., & Romaniello, M. 1999, A&A, 345, 499

Chernoff, D. F., & Weinberg, M. D. 1990, ApJ, 351, 121
Côté, P., & Fischer, P. 1996, AJ, 112, 565
Davies, M. B. 1995, MNRAS, 276, 887
Duquennoy, A., & Mayor, M. 1991, A&A, 248, 485
Eggleton, P. P., Fitchett, M., & Tout, C. A. 1989, ApJ, 347, 998
Ferraro, F. R., Paltrinieri, B., Rood, R. T., & Dorman, B. 1999, ApJ, 522, 983
Giersz, M., & Heggie, D. C. 1997, MNRAS, 286, 709
Goodman, J. 1987, ApJ, 313, 576
Han, Z. 1998, MNRAS, 296, 1019

Han, Z., Podsiadlowski, Ph., & Eggleton, P. P. 1994, MNRAS, 270, 121
Hansen, B. M. S. 1998, Nature, 394, 860
———. 1999, ApJ, 520, 680
Hansen, B. M. S., et al. 2002, ApJ, 574, L155
Harris, W. E. 1996, AJ, 112, 1487
Heggie, D. C. 1975, MNRAS, 173, 729
Hurley, J. R., Pols, O. R., & Tout, C. A. 2000, MNRAS, 315, 543
Hurley, J. R., & Shara, M. M. 2002a, ApJ, 565, 1251
———. 2002b, ApJ, 570, 184
Hurley, J. R., Tout, C. A., Aarseth, S. J., & Pols, O. R. 2001, MNRAS, 323, 630
Hurley, J. R., Tout, C. A., & Pols, O. R. 2002, MNRAS, 329, 897
Iben, I., Jr., & Livio, M. 1993, PASP, 105, 1373
Iben, I., Jr., & Tutukov, A. V. 1984, ApJ, 282, 615
Jeffries, R. D. 1997, MNRAS, 288, 585
Kalirai, J. S., Ventura, P., Richer, H. B., Fahlman, G. G., Durrell, P. R., D'Antona, F., & Marconi, G. 2001a, AJ, 122, 3239
Kalirai, J. S., et al. 2001b, AJ, 122, 257
———. 2001c, AJ, 122, 266
King, I. R. 1966, AJ, 71, 64
Koester, D. 2002, A&A Rev., 11, 33
Kroupa, P. 1995, MNRAS, 277, 1491
Kroupa, P., Tout, C. A., & Gilmore, G. 1991, MNRAS, 251, 293
———. 1993, MNRAS, 262, 545
Makino, J., & Taiji, M. 1998, Scientific Simulations with Special-Purpose Computers—the GRAPE Systems (New York: Wiley)
Maxted, P. F. L., Marsh, T. R., & Moran, C. K. J. 2002, MNRAS, 332, 745
McCook, G. P., & Sion, E. M. 1999, ApJS, 121, 1
Mestel, L. 1952, MNRAS, 112, 583
Meylan, G., & Heggie, D. 1997, A&A Rev., 8, 1

Montgomery, K. A., Marschall, L. A., & Janes, K. A. 1993, AJ, 106, 181
Nelemans, G., Yungelson, L. R., Portegies Zwart, S. F., & Verbunt, F. 2001, A&A, 365, 491
Nelson, C. A., & Eggleton, P. P. 2001, ApJ, 552, 664
Peterson, R. C., Rees, R. F., & Cudworth, K. M. 1995, ApJ, 443, 124
Pols, O. R., Schröder, K. P., Hurley, J. R., Tout, C. A., & Eggleton, P. P. 1998, MNRAS, 298, 525
Portegies Zwart, S. F., McMillan, S. L. W., Hut, P., & Makino, J. 2001, MNRAS, 321, 199
Renzini, A., et al. 1996, ApJ, 465, L23
Richer, H. B., Fahlman, G. G., Rosvick, J., & Ibata, R. 1998, ApJ, 504, L91
Richer, H. B., et al. 1996, in ASP Conf. Ser. 90, The Origins, Evolution and Destinies of Binary Stars in Clusters, ed. E. F. Milone & J.-C. Mermilliod (San Francisco: ASP), 65
———. 2002, ApJ, 574, L151
Rosvick, J. M., & VandenBerg, D. 1998, AJ, 115, 1516
Salpeter, E. E. 1955, ApJ, 121, 161
Schmidt, M. 1959, ApJ, 129, 243
Shara, M. M., & Hurley, J. R. 2002, ApJ, 571, 830
Tout, C. A. 1991, MNRAS, 250, 701
Tout, C. A., Aarseth, S. J., Pols, O. R., & Eggleton, P. P. 1997, MNRAS, 291, 732
Vesperini, E., & Heggie, D. C. 1997, MNRAS, 289, 898
von Hippel, T. 1998, AJ, 115, 1536
von Hippel, T., & Gilmore, G. 2000, AJ, 120, 1384
von Hippel, T., Gilmore, G., & Jones, D. H. P. 1995, MNRAS, 273, L39
Weidemann, V. 1987, A&A, 188, 74
Zoccali, M., et al. 2001, ApJ, 553, 733